NASA Technical Paper 1802

Performance of a Haynes 188® Metallic Standoff Thermal Protection System at Mach 7

Don E. Avery

APRIL 1981

NASA

NASA Technical Paper 1802

Performance of a Haynes 188® Metallic Standoff Thermal Protection System at Mach 7

Don E. Avery
Langley Research Center
Hampton, Virginia

National Aeronautics
and Space Administration

**Scientific and Technical
Information Branch**

1981

SUMMARY

A flight-weight, metallic thermal protection system (TPS) model applicable to reentry and hypersonic vehicles was subjected to multiple cycles of both radiant and aerothermal heating in order to evaluate its aerothermal performance and structural integrity. The TPS is a mass-optimized (9.471 kg/m^2) shingled, radiative thermal protection system constructed of Haynes alloy No. 188[1], a cobalt-base alloy. The TPS model, designed for a maximum operating temperature of 1255 K, consists of a corrugation-stiffened corrugated-skin heat shield, insulation, and beaded support ribs. The insulation package for the Haynes 188 model consists of 4.34 cm of Micro-Quartz[2] and 1.37 cm of TG 15000[3].

The Haynes 188 TPS model was subjected to 15 radiant heating tests, 3 differential pressure checkouts, and 3 radiant preheat/aerothermal tests. The tests were conducted in the Langley 8-Foot High-Temperature Structures Tunnel with the corrugations aligned in the stream direction. Wind-tunnel test conditions were at local Mach numbers of 6.7 and 4.5 with a total temperature of 1700 K and dynamic pressures of 65.0 and 63.2 kPa, respectively. The model was exposed to a hypersonic stream for a total of 67 seconds and maintained at the maximum operating temperature (1255 K) by the radiant heaters for a total of 85.9 minutes. Differential pressures across the thermal protection system ranged from 18.3 kPa (pushing in on the model) to -10.9 kPa (pushing out on the model).

The TPS limited the primary structure to temperatures below 430 K in all tests. No catastrophic failures occurred in the heat shields, supports, or insulation system; and the TPS continued to function even after exposure to a differential temperature 4 times the design value produced thermal buckles in the outer skin. The model also survived failure of the leading-edge fairing during a hypersonic stream exposure and particle impacts. The shingled thermal expansion joint effectively allowed for thermal expansion of the heat shield without allowing any appreciable hot gas flow into the model cavity, even though the overlap gap between shields increased after several thermal cycles.

INTRODUCTION

Future hypersonic cruise and reentry vehicles will require lightweight, durable thermal protection systems (TPS). The Langley Research Center has been conducting a broad-based program to advance the state of the art for metallic TPS technology because of the inherent durability of such systems. Past investigations (refs. 1 to 4) have demonstrated the feasibility of shingled, radia-

---

[1]Haynes Alloy No. 188: Registered trademark of Cabot Corporation.
[2]Micro-Quartz: Registered trademark of Johns-Manville Corporation.
[3]TG 15000: Registered trademark of HITCO.

tive metallic TPS; however, early metallic systems were heavier (ref. 4) than the fused silica reusable surface insulation (ref. 5) currently being used by the Space Shuttle Orbiter. Therefore, recent studies have focused on mass optimization, and low-mass Haynes 188 (cobalt-base alloy) and René 41 (nickel-base alloy) TPS have been designed and fabricated (ref. 6). The Haynes 188 TPS is designed for operation at temperatures up to 1255 K. The René 41 TPS provides a lower mass system for temperatures below 1144 K. The area where a Haynes 188 TPS could be applicable on the Space Shuttle Orbiter is shown in figure 1. Testing of the Haynes 188 TPS is the subject of this report.

A model representative of the Haynes 188 TPS is shown in figure 2; design details are shown in figure 3. The concept features a corrugation-stiffened corrugated-skin heat shield, beaded support ribs, and insulation. This concept represents a 35.4-percent reduction in mass over a similar Haynes alloy No. 25[4] design (ref. 1).

The aerothermal performance and structural integrity of a 70- by 91-cm Haynes 188 model was evaluated in the Langley 8-Foot High-Temperature Structures Tunnel. The model was subjected to 15 radiant heating tests, 3 radiant preheat/aerothermal tests (representative of a shuttle reentry temperature history), and 3 pressure differential checkout tests. The aerothermal tests were conducted at local Mach numbers of 6.7 and 4.5 and a unit Reynolds number of approximately 5×10^6 per meter. The model was exposed to differential pressures ranging from -10.9 kPa to 18.3 kPa.

Certain commercial materials are identified in this paper in order to adequately specify which materials were investigated during the research effort. In no case does such identification imply recommendation or endorsement of these products by NASA, nor does it imply that the materials are necessarily the only ones or the best ones available for the purpose. In many cases, equivalent materials are available and would probably produce equivalent results.

SYMBOLS

Values are given in SI units. Measurements and calculations were made in U.S. Customary Units.

D	deflection, cm
M_ℓ	local Mach number
q	dynamic pressure, kPa
R	unit Reynolds number, per meter
T	temperature, K

[4]Haynes alloy No. 25: Registered trademark of Cabot Corporation.

$T_{t,c}$ total temperature in combustor, K

t time, s

α angle of attack, deg

Δp differential pressure, kPa

ϕ center line

Abbreviations:

max maximum

ref reference

reqd required

typ typical

APPARATUS AND TESTS

Thermal Protection System

The thermal protection system (TPS) model was designed and fabricated by the Grumman Aerospace Corporation under contract to the NASA Langley Research Center. The design was based on proven baseline concepts with mass optimization as the major concern (ref. 6).

Design criteria.- The Haynes 188 TPS is designed to protect the primary structure from high surface temperatures typical of those expected during the 100 reentry cycles of the Space Shuttle Orbiter. The boost and reentry profiles for surface temperature and differential pressure used in the design of the Haynes 188 TPS (ref. 6) are shown in figure 4. These profiles correspond to reentry trajectory 14040, and the design point is located approximately 508 cm from the nose of the vehicle. For the boost phase, a maximum surface temperature of 589 K is reached 120 s after launch. A maximum negative differential pressure of -20 kPa is experienced at a lower surface temperature. During the reentry phase, a maximum surface temperature of 1255 K is reached after 500 s and is maintained for approximately 500 s before decreasing to about 300 K at 2200 s. The TPS is required to restrict the temperature of the primary structure to 450 K. The maximum positive differential pressure during peak heating will be approximately 4.78 kPa; however, a higher differential pressure (17.5 kPa) occurs at much lower surface temperatures.

General description.- The Haynes 188 TPS is a shingled, radiative thermal protection system and is designed for operation at 1255 K. The concept features a corrugation-stiffened corrugated-skin heat shield, beaded support ribs, and fibrous insulation. The heat shield of the model used in this test series to represent the Haynes 188 TPS consists of a full-size active test heat shield and a shortened fairing heat shield. Design details of the model are shown in

figure 3. Descriptions of the TPS elements also apply to the model. Table I shows the mass breakdown of each Haynes 188 TPS element and the mass savings over the original baseline design (ref. 6). The actual mass of the TPS is 9.471 kg/m^2, which is 35.4 percent of the baseline design. The mass was reduced by decreasing the skin thickness from 0.025 cm to 0.0145 cm, decreasing the number of lower clips and attachment hardware, eliminating foil bagging and support hardware for the insulation system, and using a low-density TG 15000 insulation next to the primary structure.

The geometry of the heat shield (corrugated skin and corrugated stiffener) is shown in figure 5. The corrugated outer sheet is 0.015-cm thick and has a cross-sectional shape composed of a series of circular arc segments separated by flats. This shape allows for the lateral thermal expansion of the heat shield without appreciable effect on adjacent panels. The corrugated stiffeners are trapezoidal and originally had a thickness of 0.038 cm. However, to reduce mass, the sidewalls were chem-milled to 0.0145 cm. To provide uniformity of stress, the bottoms of the stiffeners were sculptured by chem-milling. The sculptured areas of the stiffeners are represented by the dark regions in figure 6. The corrugated skin is attached to the stiffeners by three rows of overlapping spot-welds along all the flats. Buckling and creep are critical design parameters that were taken into account in the design of the TPS heat shield. Lateral thermal expansion and corrugation flutter are also critical factors in the corrugation design of the outer skin. Details of these parameters and the design conditions under which they apply are given in reference 6.

Since the aerodynamic skin expands during heating, an expansion joint is required at one transverse edge of the heat shield to permit relative motion of adjacent heat shields without allowing excessive ingress of boundary-layer air. (See fig. 3.) A shingle-slip joint concept is used at the expansion joint with the corrugated skins overlapping 1.6 cm. Because adjacent skins are mounted at the same height, an interference of 1 skin thickness was used at the faying surface to minimize leakage.

The heat shield is supported 7.32 cm off the primary structure by beaded support ribs (fig. 7). The ribs must transfer aerodynamic and heat-shield inertial loads to the primary structure with a minimum heat short. Two types of ribs were used to support the heat shield: a flexible type (fig. 7(a)) at the expansion joint (fig. 2) and a fixed type (fig. 7(b)) at the point where two adjacent heat shields butt (fig. 2). In addition to transmitting loads to the primary structure, the flexible rib also allows for longitudinal expansion of the heat shield at the expansion joint. Because the support ribs cannot react to loads in either the longitudinal or drag direction, a drag support (fig. 7(b)) is employed at 30.48-cm intervals along the fixed rib to transfer these loads to the primary structure.

The support ribs are made up of a web and clips which attach the web to the heat shield and primary structure. Although the ribs are functionally different, a common web design was developed to reduce costs. The details of the web and rib construction are given in figure 8. Web and clip thicknesses were 0.023 and 0.112 cm, respectively. The fixed and flexible ribs were attached to the heat shield and primary structure in the manner shown in figure 9. Bolts with a thermal insulation washer made of a glass-reinforced silicone laminate were used

to attach support ribs to the primary structure. Haynes 188 blind rivets were used to attach the ribs to the heat shield.

Edge fairings (figs. 3 and 9(a)) were designed to seal the test specimen within the test cavity of the panel holder and to provide a smooth surface for the aerodynamic flow during testing. The forward and aft fairings were formed with corrugations identical to those used for the heat shield. The corrugations were closed out at one end to provide a smooth surface for the aerodynamic flow. The side fairings have flat flanges spot-welded to the heat shield. All the edge fairings were formed with a curved (half-circle) lip designed to support a braided ceramic rope-type seal (fig. 9(a)).

The insulation system (fig. 10) provides the main barrier to heat transfer from the hot heat shield to the vehicle primary structure. The insulating materials consisted of 4.83 cm of Micro-Quartz and 1.52 cm of TG 15000 which were compressed by 10 percent to fit into the area between the heat shield and primary structure. This 10-percent compression of the insulation has an insignificant effect on the thermal properties, provides better retention of the insulation blanket, and compensates for the slight shrinkage which occurs after repeated high-temperature exposure. A thin aluminum insulation restraint (fig. 9(a)) was used at the leading and trailing edges of the model to hold the insulation between the fixed ribs and the model edges in place. This restraint was not part of the actual TPS design. Additional thermal protection was provided by packing the expansion cavity between the flexible ribs with Micro-Quartz insulation; however, insulation was not placed between the corrugated stiffeners of the heat shield.

Instrumentation.- The model was instrumented with 53 thermocouples and one deflectometer. Motion-picture cameras were used for photographing the panel during the wind-tunnel tests, and still photography was used for recording model surface appearance throughout the test series.

The deflectometer and thermocouple locations are shown in figure 11 and table II. Eight 30-gage chromel-alumel fiberglass-insulated thermocouples monitored the temperature of the aluminum primary structure. These thermocouples were attached to the primary structure with a high-temperature adhesive. Ceramo-chromel-alumel thermocouples were used on the heat shield, supports, and insulation. To evaluate temperature gradients through the insulation thickness, four thermocouples were distributed 1.27 cm apart through the depth at two locations (see section A-A in fig. 11); one location was the test heat-shield center, and the other was near the flexible rib. Expansion joint leakage was evaluated by three thermocouples placed in line under the skin in the expansion joint area, with the center thermocouple expected to record a higher temperature if leakage should occur. This arrangement was employed at three locations in the expansion joint area. The remaining thermocouples were spot-welded to the heat shield and support system. Because thermal expansion loops were not included in the thermocouple installation, approximately 40 percent of the thermocouples became inoperative during the tests.

Deflections were measured at the midspan of the test heat shield by a cable-type linear-displacement deflectometer capable of operating in a 477 K environment with a resolution of 0.003 cm. Basically, the deflectometer is a

potentiometer driven by the displacement of the extending cable. The deflectometer was mounted below the primary structure.

Panel Holder

General description.- The Haynes 188 TPS model was mounted in a panel holder (figs. 12 and 13) which can accommodate test models up to 152 by 108 cm (see refs. 7 and 8) for wind-tunnel testing. The aerodynamic surface of the panel holder is covered with 2.54-cm-thick low-conductivity Glasrock[5] tiles which provide thermal protection for the internal structure. A sharp leading edge with a lateral row of boundary-layer trips is used to promote a turbulent boundary layer, and aerodynamic fences provide uniform two-dimensional flow over the entire aerodynamic surface. Surface pressures and aerodynamic heating rates are varied by pitching the panel holder to a predetermined angle of attack. Differential pressure loading Δp across the heat shield is controlled by regulating the panel-holder cavity pressure under the model. (The venting around the model primary structure is sufficient to equalize the pressure in the model insulation cavity and the panel-holder cavity.) A negative Δp across the heat shield (pushing out on the model surface) is obtained by pressurizing the cavity with nitrogen, and a positive Δp (pushing in on the model surface) is obtained by venting the cavity to the lower pressure on the lee side of the panel holder.

The model was installed in the panel holder by bolting the aluminum primary structure to the sidewalls of the panel-holder interface system. Insulation washers were used to thermally isolate the model primary structure from the panel holder. The model was located 115 cm from the leading edge of the panel holder. Use of a ceramic rope seal around the edge fairings (fig. 9(a)) allowed the cavity to be pressurized without affecting the surface flow conditions.

Instrumentation.- Since the model featured no pressure orifices in the heat shield, the panel holder was instrumented with four pressure transducers (fig. 13) to measure the surface pressure exerted by the hypersonic stream. Differential pressure histories were recorded between the panel-holder surface and the panel-holder cavity by use of a differential pressure gage. Additional pressure transducers were used to monitor and control the Δp system.

Facility

The TPS model was tested in the Langley 8-Foot High-Temperature Structures Tunnel (fig. 14). This tunnel is a large blowdown facility that simulates aerodynamic heating and pressure loading at a nominal Mach number of 7 and altitudes between 25 and 40 km. The high energy needed for this simulation is obtained by burning a mixture of methane and air under pressure in the combustor and expanding the products of combustion through a conical contoured nozzle into the open jet test chamber. The flow enters a supersonic diffuser

---

[5]Glasrock: Trade name of Glassrock Products.

where an air ejector pumps it through a mixing tube and exhausts it to the atmosphere through a subsonic diffuser. This tunnel operates at combustor total temperatures $T_{t,c}$ from 1400 to 2000 K, at combustor total pressures from 4.1 to 24.1 MPa, and at free-stream unit Reynolds numbers from 1.0×10^6 to 10.0×10^6 per meter.

The test model is initially covered with acoustic baffles and stored in a pod below the test stream (fig. 14(b)) to protect it from adverse tunnel-startup transient and acoustic loads. Once the desired flow conditions are established, the baffles are retracted and the model is rapidly inserted into the test stream (fig. 14(c)) on a hydraulically actuated elevator. A model pitch system provides an angle-of-attack range of $\pm 20^{\circ}$.

A radiant heater system was used for both the radiant heating tests and as a preheat for the aerothermal tests. This radiant heater system consists of quartz-lamp radiators mounted on the acoustic baffles (fig. 14). The radiant lamps are powered by an ignitron tube power supply and are controlled by a closed-loop servo system to produce the desired temperature histories. More detailed information concerning the test facility can be found in references 7 and 8.

Tests

The Haynes 188 TPS model was subjected to radiant heating tests and radiant preheat/aerothermal tests with temperature-time histories similar to those shown in figure 4 for the Space Shuttle. Appropriate differential pressures were also applied during model testing. In both the radiant heating and the aerothermal tests, radiant lamps were used to heat the model to the maximum operating temperature at a rate of 2.0 K/s. Figure 15 shows a typical radiant or radiant preheat/aerothermal heating profile simulating reentry conditions. During radiant heating tests, the temperature profile was the same except that the aerothermal portion was deleted. A few tests were conducted near the beginning of the test series to check the model and test equipment at lower thermal loads.

The Haynes 188 TPS model was exposed to a total of 21 tests: 15 radiant heating tests, 3 Δp checkouts, and 3 radiant preheat/aerothermal tests. The maximum temperatures, time exposed to maximum temperature, and Δp across the model for each type of test are listed in table III. Incomplete radiant heating tests are included to show exactly what conditions the model experienced. Table IV lists the pertinent wind-tunnel test conditions. The local Mach numbers M_{ℓ} were nominally 6.7 and 4.5, and an approximate local Reynolds number of 5×10^6 per meter was obtained. The free-stream dynamic pressures were 65.0 and 63.2 kPa.

Several events which subjected the model to unusual load conditions occurred during the test series. During test 4, the model was inadvertently overloaded to 18.34 kPa. During radiant heating tests 9 and 12, the model was heated at a rate higher than desired because thermocouples used to control the model temperature were lost at the start of the run. During test 21, the leading-edge fairing failed. The leading-edge fairing functions as an interface between the

heat shield and the panel holder and is not part of the actual TPS design. More details of these events are presented in "Results and Discussion."

Test Procedures and Data Reduction

Test 1 simulated the high Δp, low-temperature boost trajectory (fig. 4(a)). This test involved heating the model at a rate of 2.0 K/s to 590 K, applying the expected Δp, maintaining this condition, and then releasing the Δp while cooling the model at a rate of 2.0 K/s until natural cooling occurred. The remaining heating tests were representative of a Space Shuttle Orbiter reentry trajectory (fig. 4(b)). During most of the tests, the temperature of the heat shield was raised to the maximum operating temperature (1255 K) using the radiant heaters. For the radiant heating tests (fig. 15), the maximum surface temperature was maintained for periods up to approximately 500 s and then allowed to follow the remainder of the expected Shuttle trajectory until the natural cooling rate was less than 2 K/s. For the radiant preheat/aerothermal tests (fig. 15), the maximum preheat temperature was maintained for approximately 500 s prior to wind-tunnel exposure. When wind-tunnel flow conditions capable of maintaining the desired temperature were stabilized, the model was quickly exposed to the hypersonic stream for as long as test conditions could be maintained. (See table III.) The aerothermal exposure could be programmed to occur at any point during the simulated Shuttle trajectory.

The procedure for the aerothermal part of the tests was to start the tunnel, obtain correct flow conditions, deenergize the radiant heaters, retract the heaters and acoustic baffles, and insert the model into the hypersonic stream while simultaneously pitching the panel holder. The desired angle of attack was obtained prior to reaching the stream center line. At the end of the aerothermal exposure, this procedure was reversed, and tunnel shutdown was initiated after the heaters and acoustic baffles had covered the model and the heaters had been reenergized. From this point, the heaters would continue to follow the Shuttle trajectory until the natural cooling rate was less than 2 K/s. The time lapse between the lamps being deenergized and the model entering the stream, and between the model leaving the stream and the lamps being reenergized, was kept to a minimum (approximately 5 s for each operation).

Model and tunnel instrumentation data were recorded by high-speed digital recorders. During radiant heating tests and preheat events, thermocouple, pressure, and deflectometer outputs were recorded at 2-s intervals. During the aerothermal portion of the tests, data were recorded at 20 samples per second. All data were reduced to engineering quantities at the Langley Central Digital Data Recording Facility. The analytical quantities reported for these wind-tunnel tests are based on the thermal, transport, and flow properties of the combustion products test medium as determined from reference 9. Free-stream conditions in the test section were determined from reference measurements in the combustion chamber by using results from tunnel-stream survey tests such as those reported in reference 8. The local Mach number was obtained from oblique-shock relations.

RESULTS AND DISCUSSION

Summary of TPS Tests

Results of the Haynes 188 TPS model tests are summarized in tables III and IV. The model was held at its approximate maximum operating temperature (1255 K) by radiant heaters for a total of 85.9 minutes and was exposed to a hypersonic stream for a total of 67 seconds. Figures 16, 17, and 18 describe the load environment and the response of the model during the test series.

TPS Thermal Performance

Figure 19 shows the temperature distribution through the insulation and on the primary structure for both a radiant heating test (fig. 19(a)) and a radiant preheat/aerothermal test (fig. 19(b)). During the latter test, aerothermal heating occurred between 1628 and 1646 s. The trends for radiant heating and radiant preheat/aerothermal tests are similar. For both types of tests, the maximum temperature in the insulation reached approximately 1100 K; however, the maximum primary structure temperature was approximately 420 K, which is approximately 30 K less than the design value of 450 K. The design value was based on the assumption that there was no heat loss from the backface of the primary structure (i.e. an adiabatic surface). Since the temperature of the primary structure began to decrease while the insulation was hotter than the primary structure (fig. 19), heat losses out the backface of the primary structure are significant. Thermal analyses of the model which assumed radiation and gas conduction from the primary structure backface indicate a primary structure temperature of 409 K; thus, the TPS appears to have performed essentially as expected. Figure 20 shows the temperature response of the heat shield, support, and primary structure for the same tests. At this leading-edge location, the surface temperature remained below the desired 1255 K, and the maximum primary structure temperature reached only 390 K. The maximum temperature of the primary structure may have been lower at thermocouple 5 than at thermocouple 31 (fig. 19) because thermocouple 5 is located over an I-beam flange that supports the primary structure (figs. 3 and 11). The I-beam could have conducted heat away from thermocouple 5; thus the maximum temperature was lower than at thermocouple 31. However, the I-beam also reduced the heat loss out the backface of the primary structure in the area of thermocouple 5; therefore, this thermocouple continued to rise after all the other thermocouples had reached their maximum temperature. These data show the effect of conduction down the support ribs. The maximum upper clip temperatures were approximately 1100 K, and the maximum web temperatures were approximately 1000 K, indicating high thermal conductivity. However, the primary structure temperatures (figs. 19 and 20) were approximately the same, indicating the effectiveness of the thermal washer and diffusion of the heat short by the aluminum primary structure.

An important factor in the design of metallic thermal protection systems is the effectiveness of the individual heat-shield joints in preventing hot gas flow into the TPS cavity. Past investigations have shown the shingle-slip joint to be an effective design, which permits thermal-expansion but prevents excessive hot gas ingress. Therefore, the shingle joint was used in this design.

The effectiveness of the shingle-slip joint was difficult to determine for this test series because of the extensive loss of instrumentation. However, none of the primary structure thermocouples in the area of the joint indicated a temperature over 430 K. This result indicates that there was at most a minimal ingress of hot boundary-layer gas, even though the overlap gap between shields opened to a maximum of 0.18 cm as the test series progressed.

TPS Structural Performance

Structural ruggedness of the TPS was demonstrated when the model was inadvertently subjected to several unusual load conditions. During test 4 (fig. 17), the design maximum Δp of 16.75 kPa was exceeded, and a value of Δp of 18.3 kPa was imposed on the model. There was no apparent damage to the model, although the ceramic rope seal around the model was blown out and had to be replaced. Subsequently in tests 9 and 12, the model was subjected to uncontrolled rapid heating and cooling when heater control thermocouples failed; and in test 21, the model was subjected to an ingress of hot gas and particle impingement when the leading-edge fairing failed.

The uncontrolled heating and cooling during tests 9 and 12 induced noncatastrophic thermal buckling of the heat shield. The heating rate during test 9 was twice the expected rate and resulted in a maximum temperature difference between the corrugated skin and corrugation stiffener bottom of 179 K. The heating rate during test 12 was approximately 21 times the expected rate. Although the test was terminated as soon as the problem was realized, the temperature difference between the skin and the bottom of the corrugation stiffener reached 529 K. (See fig. 21.) This temperature difference was 4 times the design temperature difference. The dashed curve in figure 21 represents the desired skin temperature for the test period of time. As a result of the temperature difference, most of the thermal buckles in figure 22 were created. Section A-A of figure 22 shows that the buckles were usually located on one side of the heat shield corrugation, running from the crest of the corrugation to the adjacent flat. The average depth of the buckle was 0.05 cm. Also, during test 12 the heat shield was deflected 1.6 cm (fig. 18) through thermal loading but sustained no apparent permanent deformation.

The Haynes 188 TPS test series was terminated after the failure of the leading-edge fairing during test 21. This leading-edge fairing, which is not part of the actual TPS test hardware, functions as an interface between the TPS and the panel holder. Early in the test series, the fairing began to buckle because of the constraint provided by the portion of fairing below the surface of the panel holder that was not exposed to direct heating (see fig. 9(a)). Gradually a crack and a forward-facing step developed (fig. 23(a)). Localized heating of the protrusion during aerothermal tests further aggravated the problem. Finally, under the more severe conditions of test 21, the fairing failed completely under the combined thermal and air loads and peeled back, permitting unrestrained hot gas ingress. Figures 23(b), (c), and (d) show the post-test condition of the model. Although the model was removed from the test stream as soon as the problem was discovered, the hot gas caused the failure of the thin aluminum insulation restraint. (See fig. 23(c).) This restraint was not part of the basic TPS design but was peculiar to the test model. The hot gas also

blew away the insulation located under the fairing as well as a small amount located behind the rib near the center of the model (figs. 23(b) and (c)).

However, this major damage apparently did not compromise the thermal or structural performance of the model. No wholesale loss of insulation occurred and post-test examination revealed no structural failure in the heat shield, clips, web, or primary structure. Measurements from the thermocouples indicated that all parts of the structure overheated in the leading-edge region; however, the maximum temperature is not known because the data were off scale. Furthermore, impingement of fragments of the leading-edge fairing (or particles from the wind-tunnel stream) during the test did not cause catastrophic failure of the trailing-edge fairing. (See fig. 23(e).)

CONCLUDING REMARKS

A flight-weight, metallic thermal protection system (TPS) model applicable to reentry and hypersonic vehicles was subjected to multiple cycles of both radiant and aerothermal heating in order to evaluate its aerothermal performance and structural integrity. The TPS, which was designed for a maximum operating temperature of 1255 K, consisted of a shingled radiative heat shield, fibrous insulation, and beaded support ribs. The corrugation-stiffened corrugated-skin heat shield and support ribs were constructed of Haynes 188, a cobalt-base alloy.

The TPS model was subjected to 15 radiant heating tests, 3 differential pressure checkouts, and 3 radiant preheat/aerothermal tests in the Langley 8-Foot High-Temperature Structures Tunnel. Wind-tunnel test conditions were at local Mach numbers of 6.7 and 4.5 with a total temperature of 1700 K and dynamic pressures of 65.0 and 63.2 kPa, respectively. The model was exposed to a hypersonic stream for a total of 67 seconds and maintained at the maximum operating temperature (1255 K) for a total of 85.9 minutes. Differential pressures across the thermal protection system ranged from 18.3 kPa (pushing in on the model) to -10.9 kPa (pushing out on the model).

The TPS limited the primary structure to temperatures below 430 K in all tests. No catastrophic failures occurred in the heat shields, supports, or insulation system, and the TPS continued to function even after exposure to a differential temperature 4 times the design value produced thermal buckles in the outer skin. The model also survived failure of the leading-edge fairing during a hypersonic stream exposure and particle impacts. The shingled thermal expansion joint effectively allowed for thermal expansion of the heat shield without allowing any appreciable hot gas flow into the model cavity, even though the overlap gap between shields increased after several thermal cycles.

Langley Research Center
National Aeronautics and Space Administration
Hampton, VA 23665
March 3, 1981

REFERENCES

1. Sawyer, James Wayne: Aerothermal and Structural Performance of a Cobalt-Base Superalloy Thermal Protection System at Mach 6.6. NASA TN D-8415, 1977.

2. Deveikis, William D.; Miserentino, Robert; Weinstein, Irving; and Shideler, John L.: Aerothermal Performance and Structural Integrity of a René 41 Thermal Protection System at Mach 6.6. NASA TN D-7943, 1975.

3. Bohon, Herman L.; Sawyer, J. Wayne; Hunt, L. Roane; and Weinstein, Irving: Performance of Thermal Protection Systems in a Mach 7 Environment. J. Spacecr. & Rockets, vol. 12, no. 12, Dec. 1975, pp. 744-749.

4. Bohon, Herman L.; Shideler, John L.; and Rummler, Donald R.: Radiative Metallic Thermal Protection Systems: A Status Report. J. Spacecr. & Rockets, vol. 14, no. 10, Oct. 1977, pp. 626-631.

5. Emde, Wendall D.: Thermal Protection System for the Shuttle Orbiter. Bicentennial of Materials Progress, Volume 21 of National SAMPE Symposium and Exhibition, Soc. Advance. Mater. & Process Eng., 1976, pp. 964-978.

6. Varisco, Angelo; Bell, Paul; and Wolter, Willy: Design and Fabrication of Metallic Thermal Protection Systems for Aerospace Vehicles. NASA CR-145313, 1978.

7. Deveikis, William D.; Bruce, Walter E., Jr.; and Karns, John R.: Techniques for Aerothermal Tests of Large, Flightweight Thermal Protection Panels in a Mach 7 Wind Tunnel. NASA TM X-71983, 1974.

8. Deveikis, William D.; and Hunt, L. Roane: Loading and Heating of a Large Flat Plate at Mach 7 in the Langley 8-Foot High-Temperature Structures Tunnel. NASA TN D-7275, 1973.

9. Leyhe, E. W.; and Howell, R. R.: Calculation Procedure for Thermodynamic, Transport, and Flow Properties of the Combustion Products of a Hydrocarbon Fuel Mixture Burned in Air With Results for Ethylene-Air and Methane-Air Mixtures. NASA TN D-914, 1962.

TABLE I.- MASS OF TPS ELEMENTS AND MASS SAVINGS

OVER ORIGINAL BASELINE DESIGN

Element	Actual mass, kg/m^2	Percent of element	Element percent of TPS	Percent change in mass between baseline and new design
Surface panel	5.2733	100.0	55.7	-25.1
Skin	1.5087	28.6	15.9	
Stiffener	3.4716	65.8	36.7	
Doublers	.1758	3.3	1.9	
Attach rivets	.1172	2.2	1.2	
Supports	1.2481	100.0	13.2	-50.3
Webs	.2637	21.1	2.8	
Upper clips	.4814	38.6	5.1	
Lower clips	.2676	21.4	2.8	
Drag brackets	.0879	7.0	.9	
Attach hardware	.1475	11.8	1.6	
Insulation	2.9496	100.0	31.1	-40.2
Micro-Quartz	2.7055	91.7	28.6	
TG 15000	.2441	8.3	2.6	
Total	9.4710		100	-35.4

TABLE II.- THERMOCOUPLE LOCATIONS

Thermocouple ID no.	Row-col[a]	Location
1	3-1	Edge seal, fairing heat shield
2	3-2	Skin, fairing heat shield
3	3-2	Clip, fairing heat shield
4	3-2	Standoff web, fairing heat shield
5	3-2	Primary structure, fairing heat shield
6	2-3	Skin, fairing heat shield
7	3-3	Skin, fairing heat shield
8	4-3	Skin, fairing heat shield
9	3-4	Clip, fairing heat shield
10	3-4	Standoff web, fairing heat shield
11	3-4	Primary structure, fairing heat shield
12	2-5	Skin, fairing heat shield
13	3-5	Skin, fairing heat shield
14	4-5	Skin, fairing heat shield
15	4-5	Clip, fairing heat shield
16	4-5	Standoff web, fairing heat shield
17	4-5	Primary structure, fairing heat shield
18	2-6	Skin, test heat shield
19	3-6	Skin, test heat shield
20	4-6	Skin, test heat shield
21	2-7	Skin, test heat shield
22	2-7	Clip, test heat shield
23	2-7	Standoff web, test heat shield
24	2-7	Primary structure, test heat shield
25	3-7	Skin, test heat shield
26	4-7	Skin, test heat shield
27	3-8	Insulation at 5.08 cm, test heat shield
28	3-8	Insulation at 3.81 cm, test heat shield
29	3-8	Insulation at 2.54 cm, test heat shield
30	3-8	Insulation at 1.27 cm, test heat shield
31	3-8	Primary structure, test heat shield
32	3-9	Skin, test heat shield
33	3-9	Stiffener bottom, test heat shield
34	1-10	Edge seal, test heat shield
35	2-10	Skin, test heat shield
36	3-10	Skin, test heat shield
37	3-10	Stiffener bottom, test heat shield
38	3-10	Insulation at 5.08 cm, test heat shield
39	3-10	Insulation at 3.81 cm, test heat shield
40	3-10	Insulation at 2.54 cm, test heat shield
41	3-10	Insulation at 1.27 cm, test heat shield
42	3-10	Primary structure, test heat shield
43	4-10	Skin, test heat shield
44	4-10	Stiffener bottom, test heat shield
45	4-10	Primary structure, test heat shield
46	5-10	Edge seal, test heat shield
47	3-11	Skin, test heat shield
48	3-11	Stiffener bottom, test heat shield
49	3-12	Skin, test heat shield
50	3-12	Clip, test heat shield
51	3-12	Standoff web, test heat shield
52	3-12	Primary structure, test heat shield
53	3-13	Edge seal, test heat shield

[a]See figure 11.

TABLE III.- SUMMARY OF TESTS

Test no.	Type of test	Maximum radiant temperature (av), K	Maximum aerothermal temperature (av), K	Time at maximum surface temperature, s		Δp, kPa	
				Radiant	Aero-thermal	-	+
1	Radiant	590		32		8.2	
2	Radiant	800		0		0	
3	Radiant	1220		12		0	
4	Δp checkout					5.4	18.3
5	Radiant	1220		518		0	
6	Δp checkout					9.3	7.5
7	Radiant	1300		545		0	
8	Δp checkout					4.2	
9[a]	Radiant	1280		147		0	
10	Radiant	1300		335		0	
11	Radiant	1190		535		10.9	4.7
12[a]	Radiant	1010		0		0	
13	Radiant	1240		510		0	
14	Aerothermal	1240	810	516	18	9.4	1.4
15	Aerothermal	1230	880	508	36	9.7	4.2
16	Radiant	1230		516		10.5	5.1
17	Radiant	1230		124		0	
18	Radiant	570		5		9.5	5.1
19	Radiant	1130		54		0	
20	Radiant	1230		314		0	
21	Aerothermal	1250	1050	493	13	10.1	6.8

[a]Rate of heating excessive.

TABLE IV.- WIND-TUNNEL TEST CONDITIONS

Test no.	$T_{t,c}$, K	α, deg	q, kPa	M_{∞}	R, per m
14	1700	0.5	65.0	6.7	5.07×10^6
15	1700	.2	65.0	6.8	5.07
21	1700	12.6	63.2	4.5	4.83

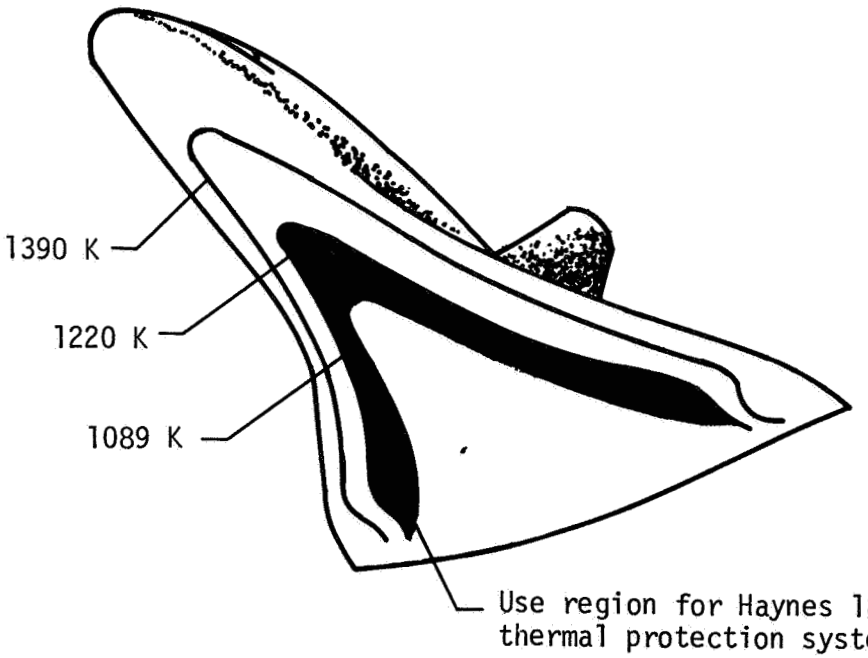

Figure 1.- Reentry isotherms on lower surface of Space Shuttle Orbiter.

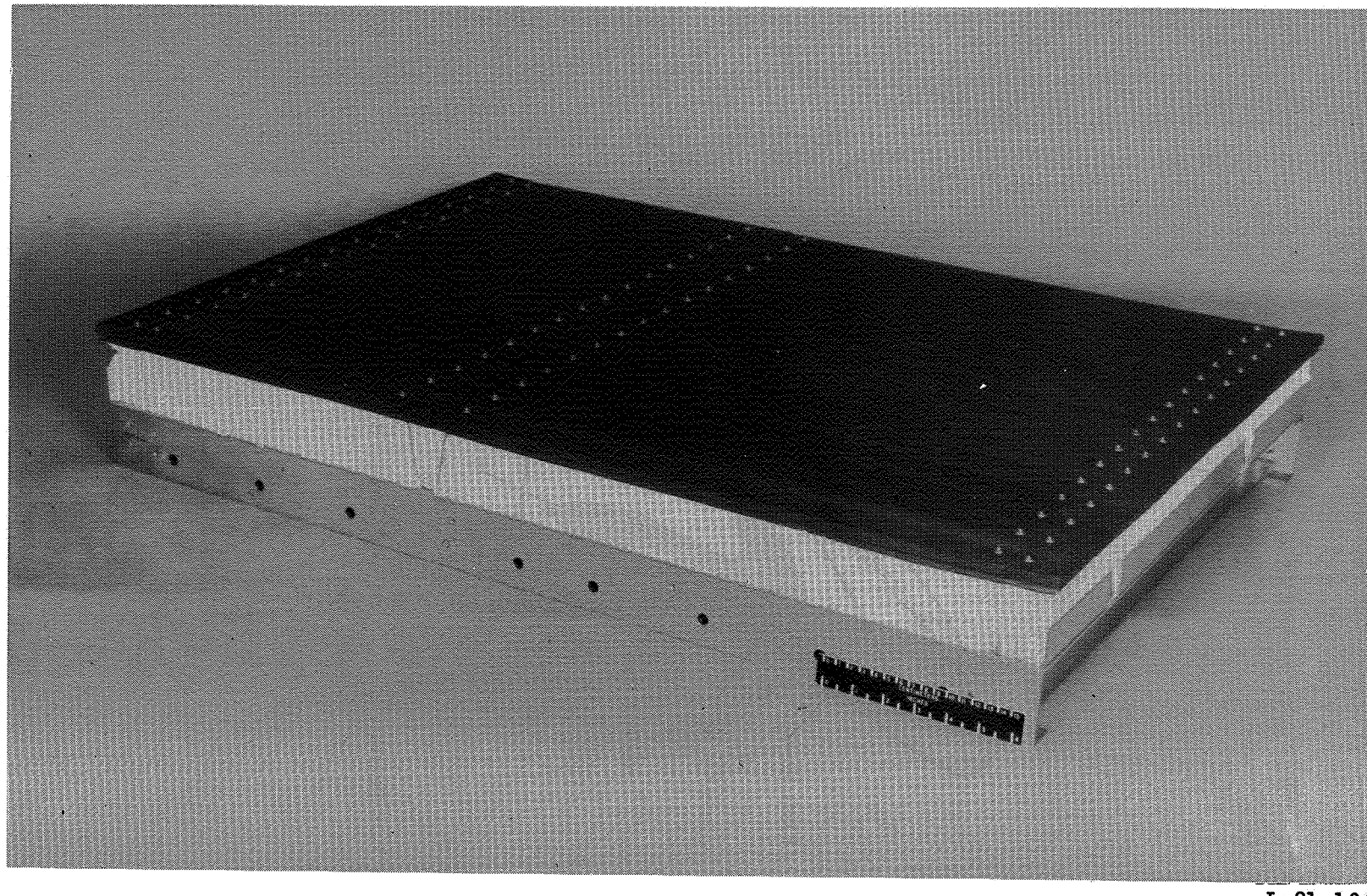

L-81-104

Figure 2.- Model of Haynes 188 thermal protection system.

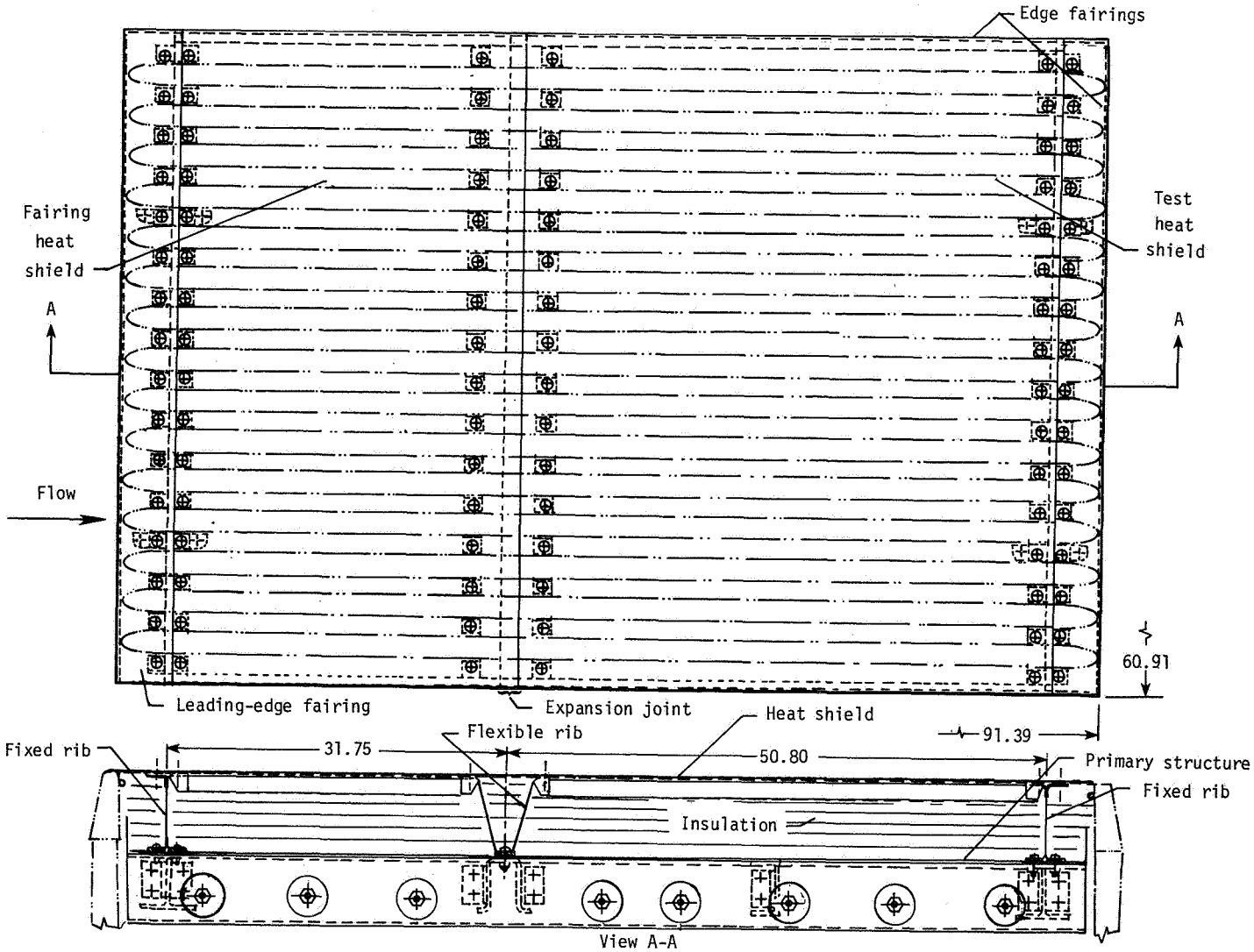

Figure 3.- Design details. Dimensions are in centimeters.

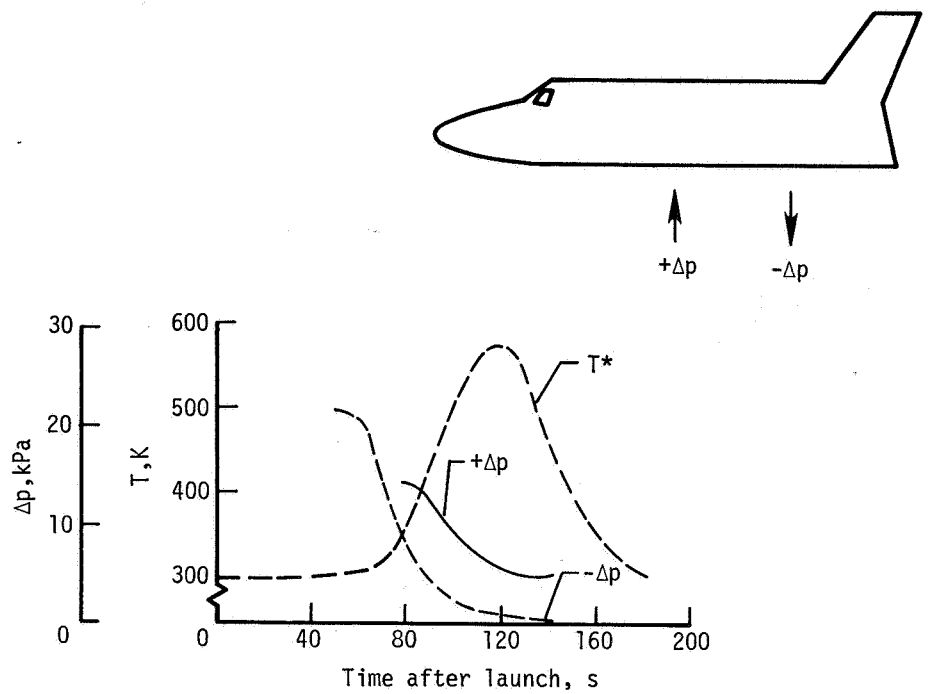

(a) Boost profile. (T* denotes temperature on lower surface approximately 508 cm aft.)

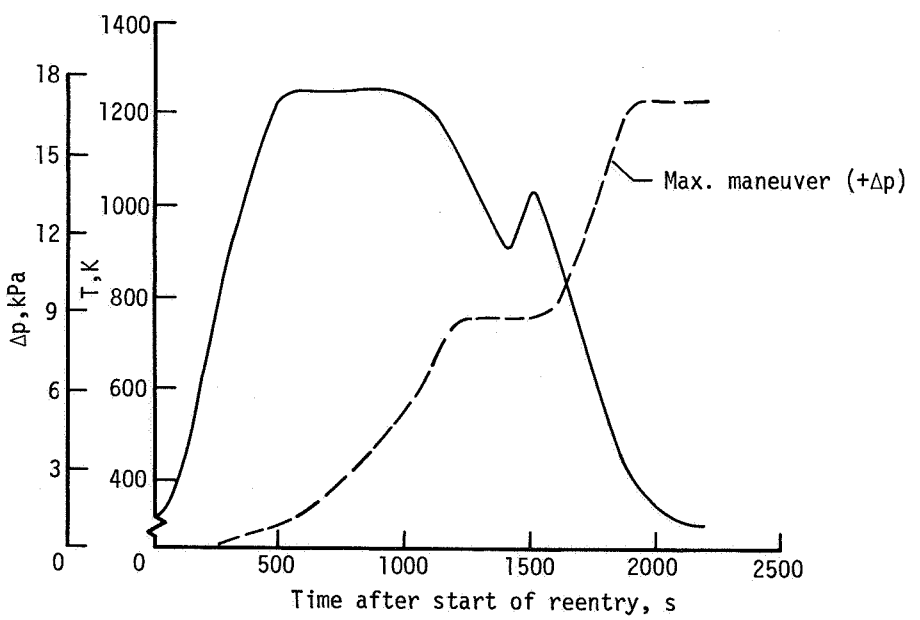

(b) Reentry profile.

Figure 4.- Temperature and pressure profiles for Space Shuttle trajectory (ref. 6).

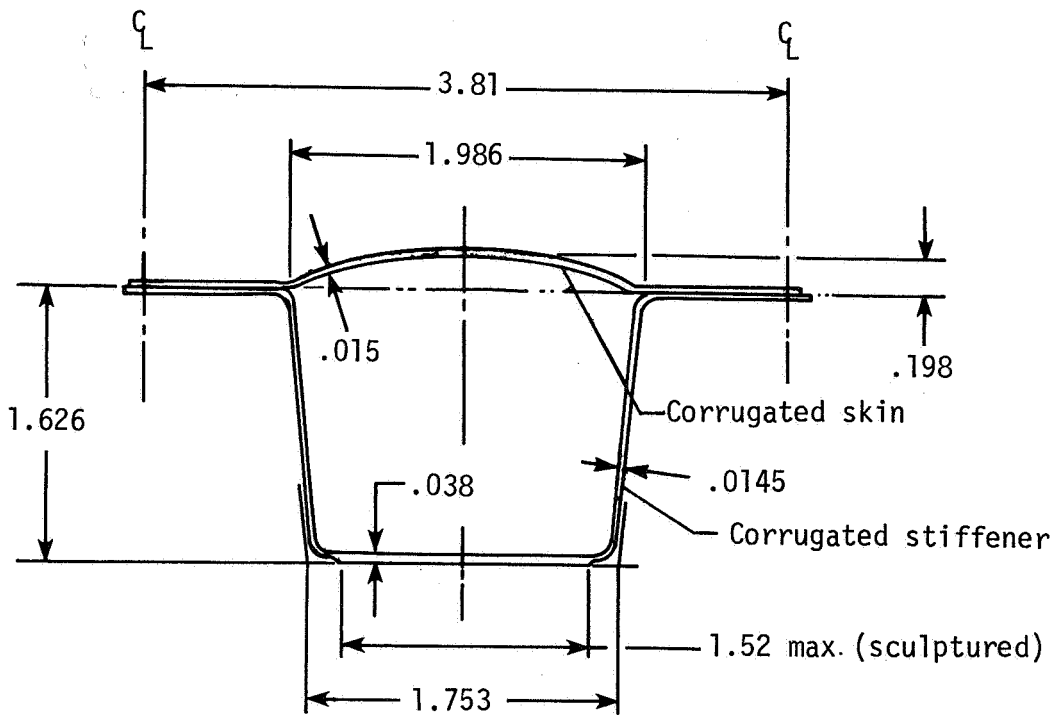

Figure 5.- Geometry of heat shield. Dimensions are in centimeters.

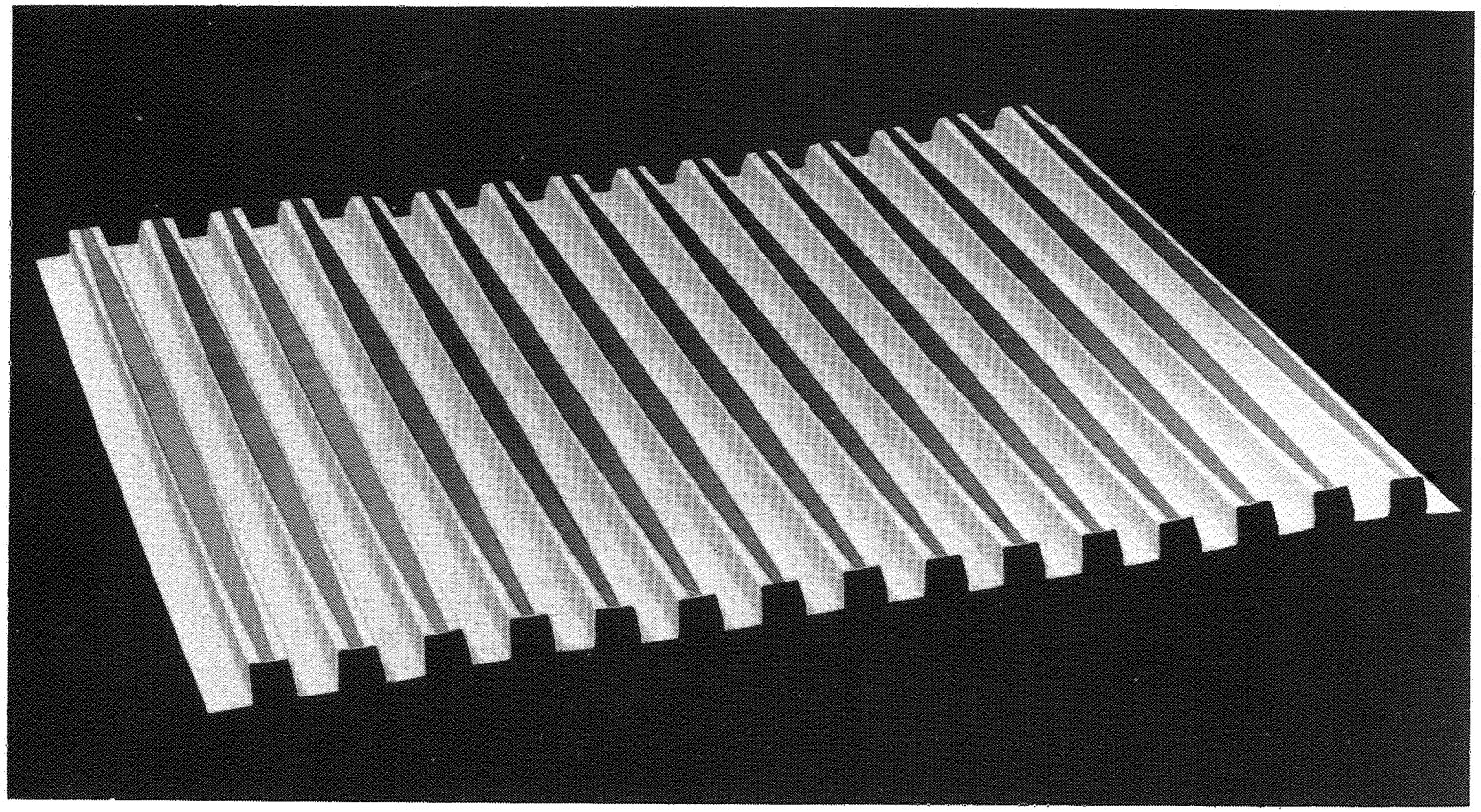

L-81-105

Figure 6.- Sculptured corrugated stiffener.

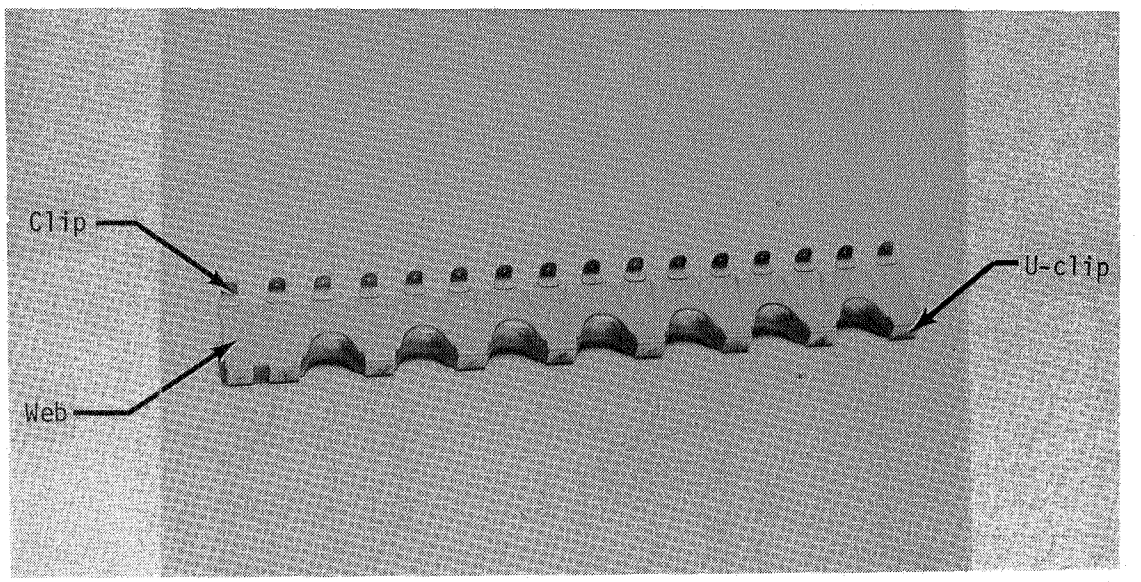

(a) Flexible rib.

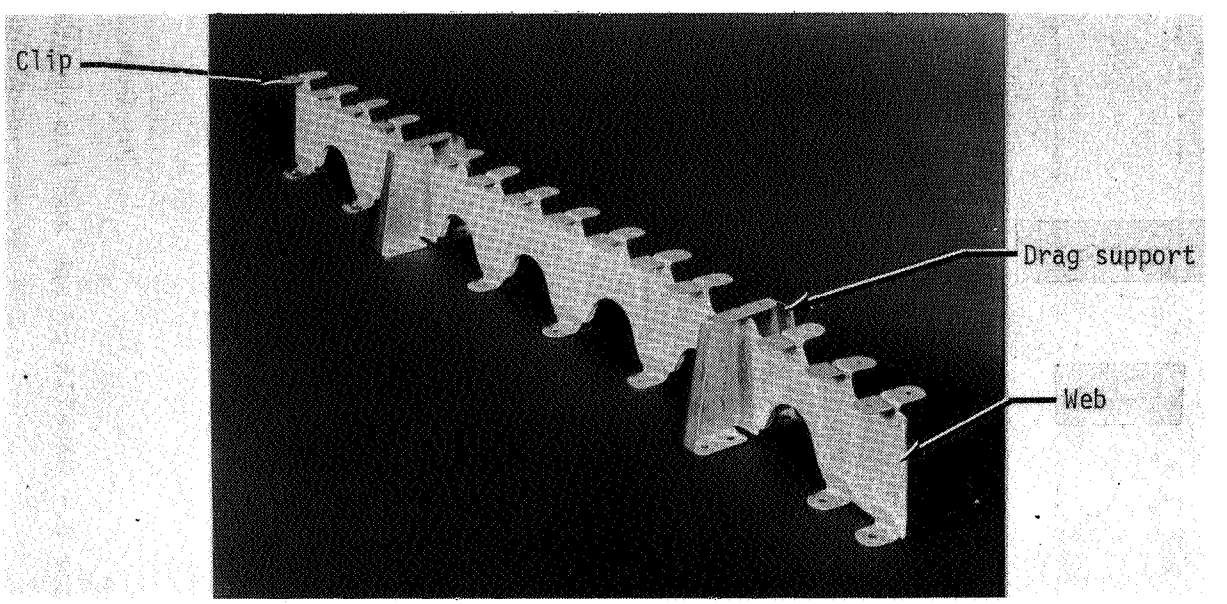

(b) Fixed rib with drag supports.

L-81-106

Figure 7.- Beaded support ribs.

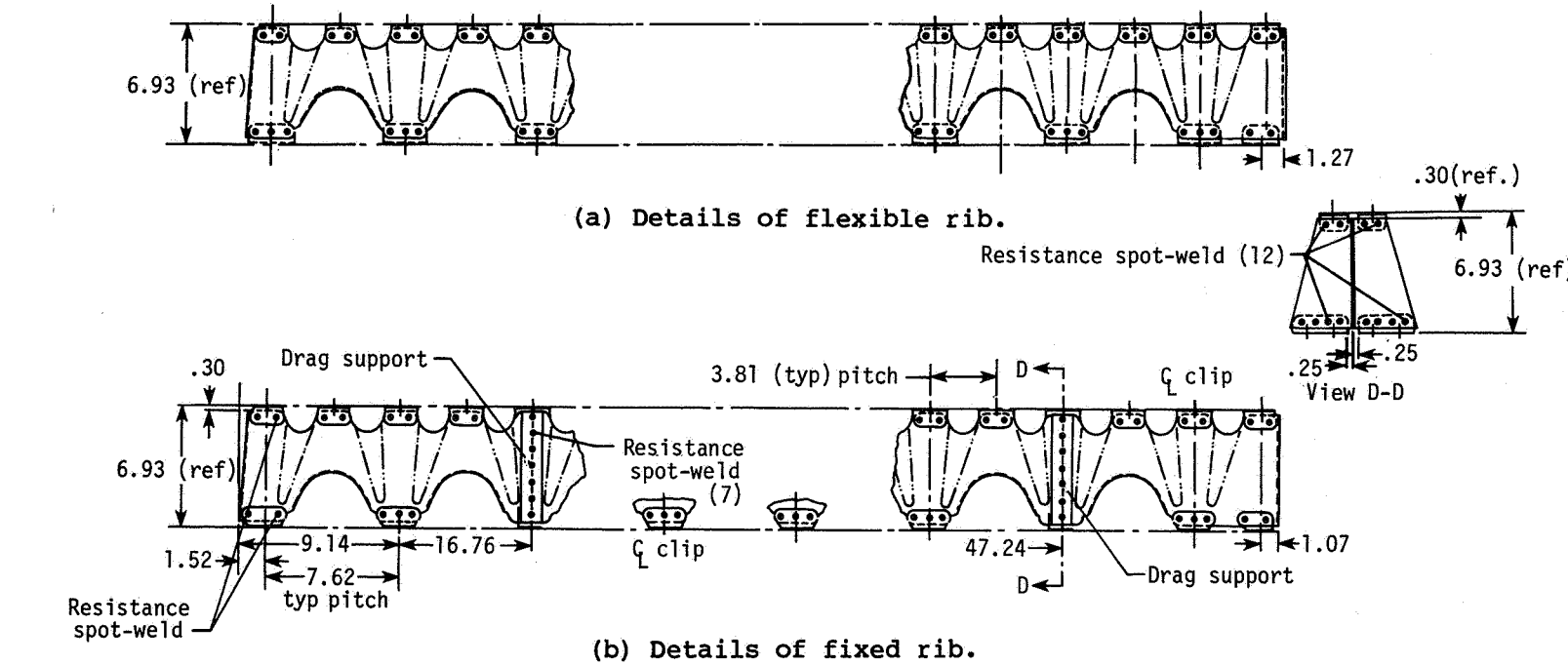

(a) Details of flexible rib.

(b) Details of fixed rib.

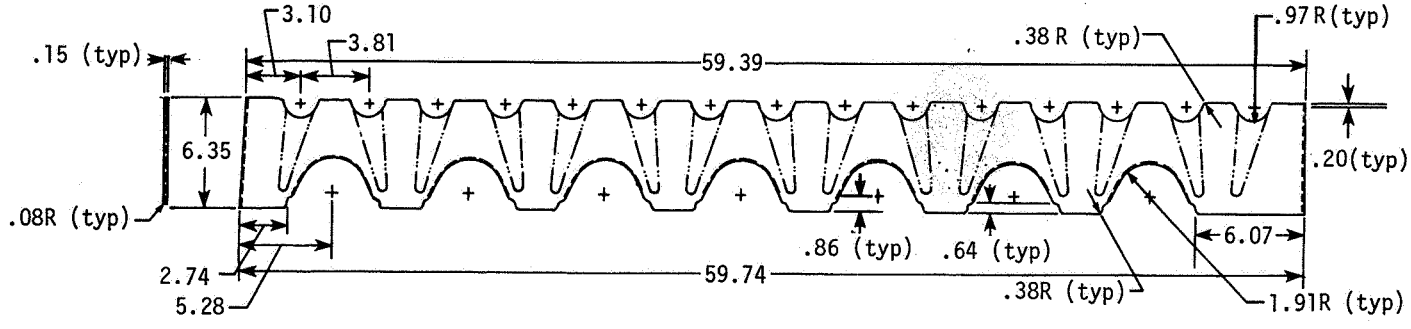

(c) Details of web.

Figure 8.- Details of web and rib construction. Dimensions are in centimeters.

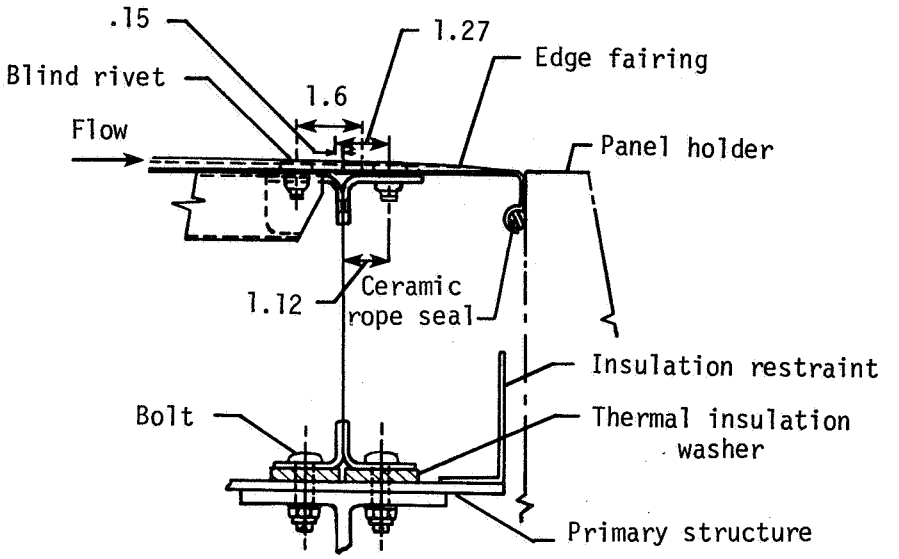

(a) Fixed rib.

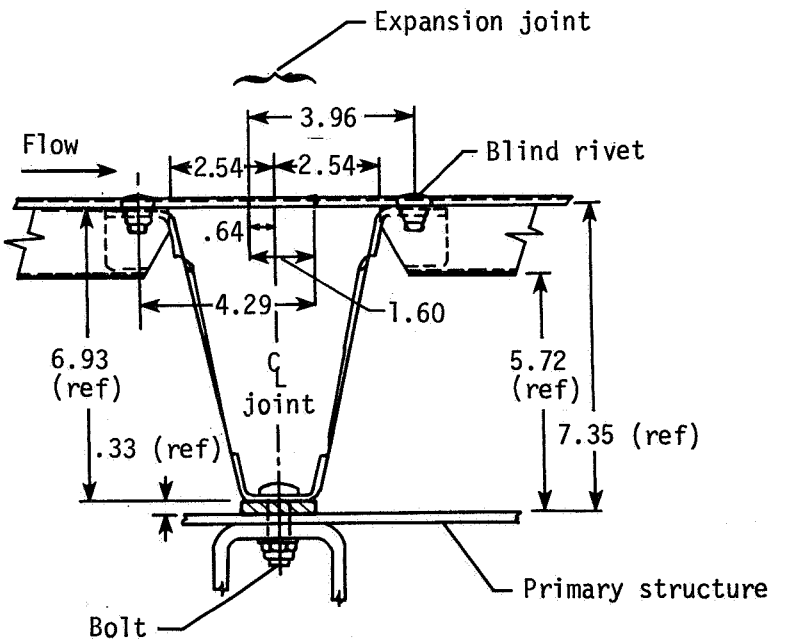

(b) Flexible rib.

Figure 9.- Details of support attachment. Dimensions are in centimeters.

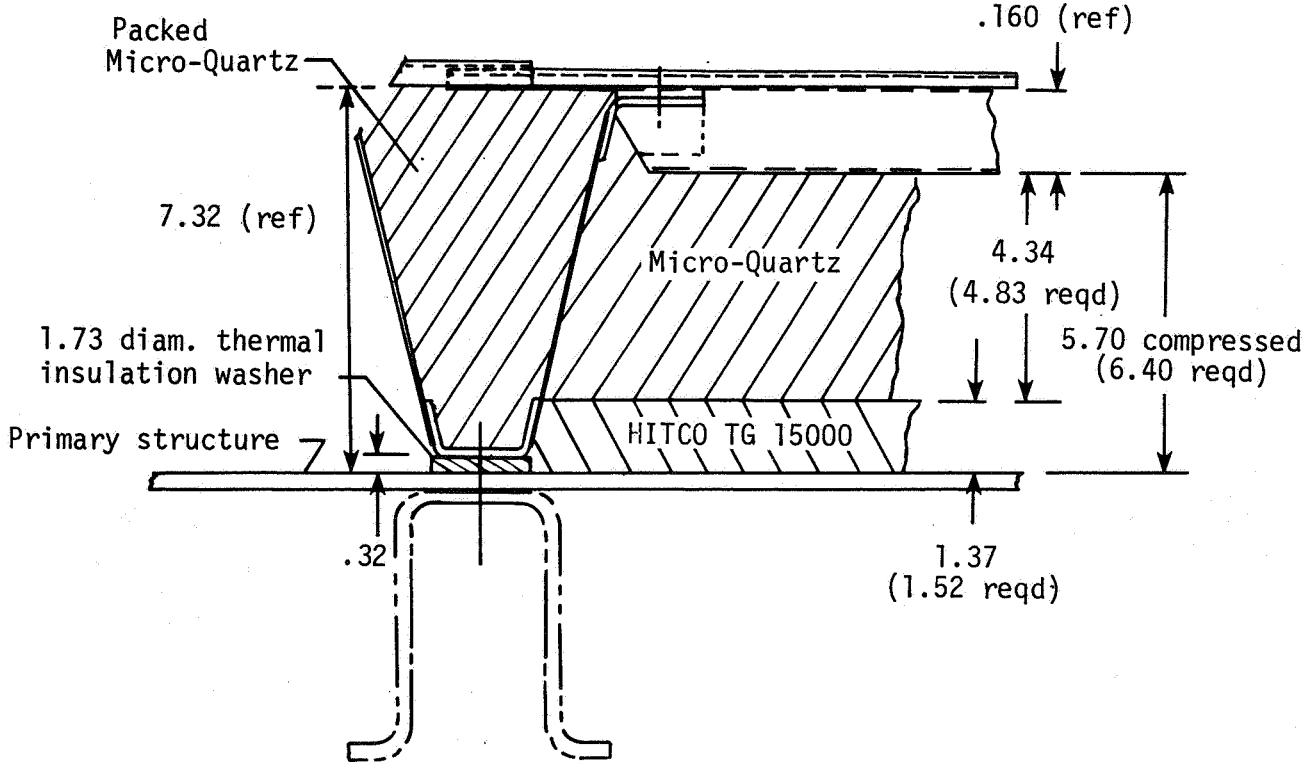

Figure 10.- Insulation system. Dimensions are in centimeters.

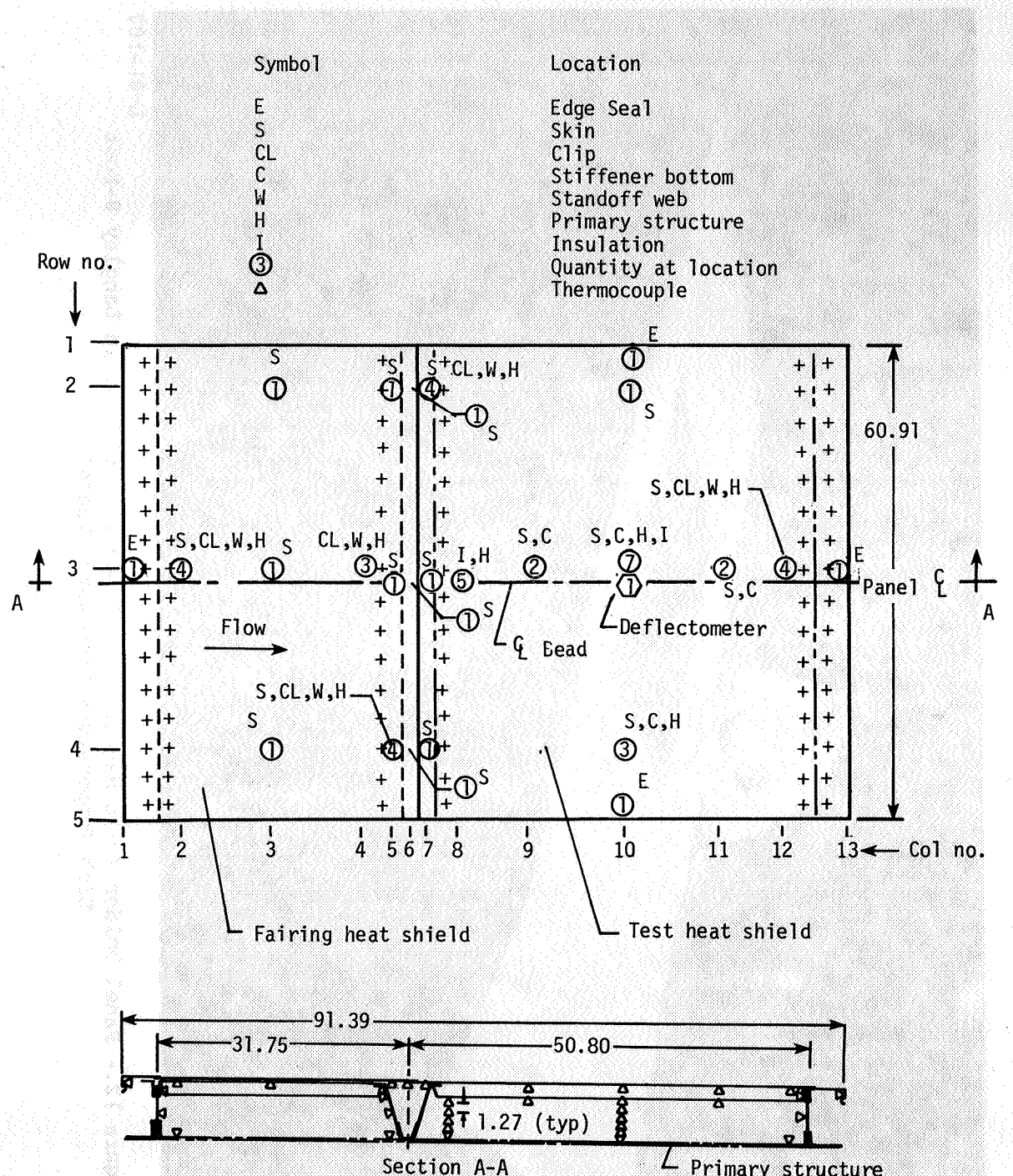

Figure 11.- Instrumentation for Haynes 188 TPS model. Dimensions are in centimeters.

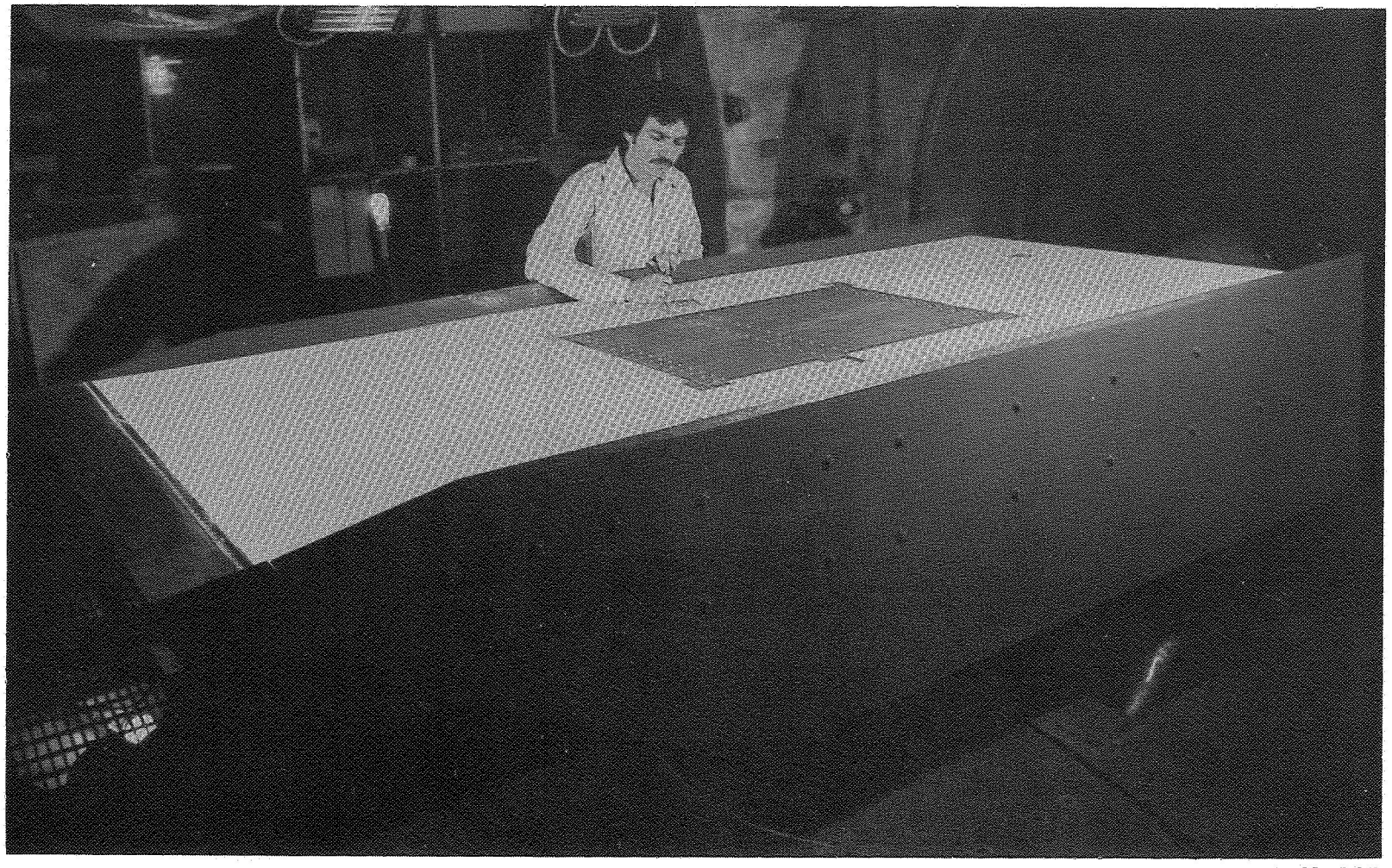

L-81-107

Figure 12.- Panel holder (with Haynes 188 TPS model installed) in Langley 8-Foot High-Temperature Structures Tunnel.

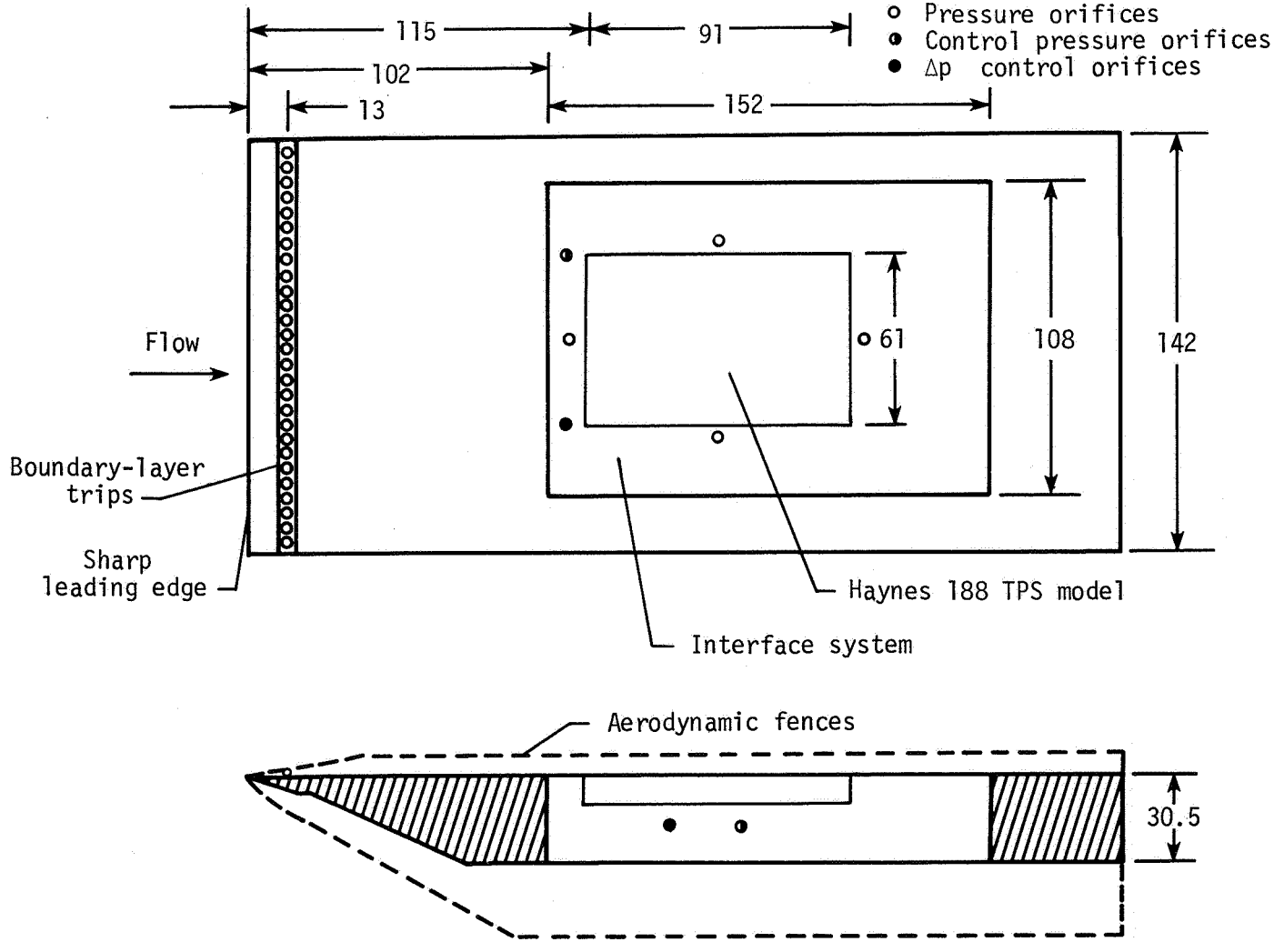

Figure 13.- Sharp leading-edge panel holder with TPS model installed. Dimensions are in centimeters.

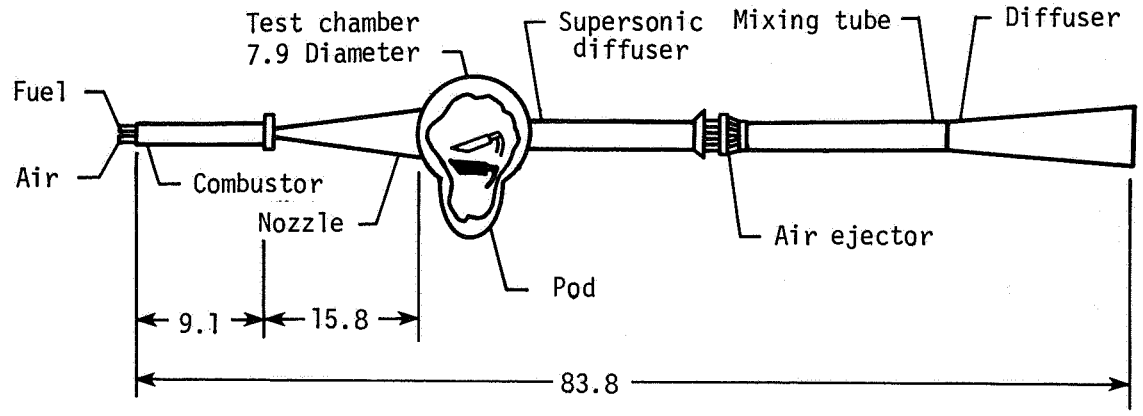

(a) Schematic of tunnel.

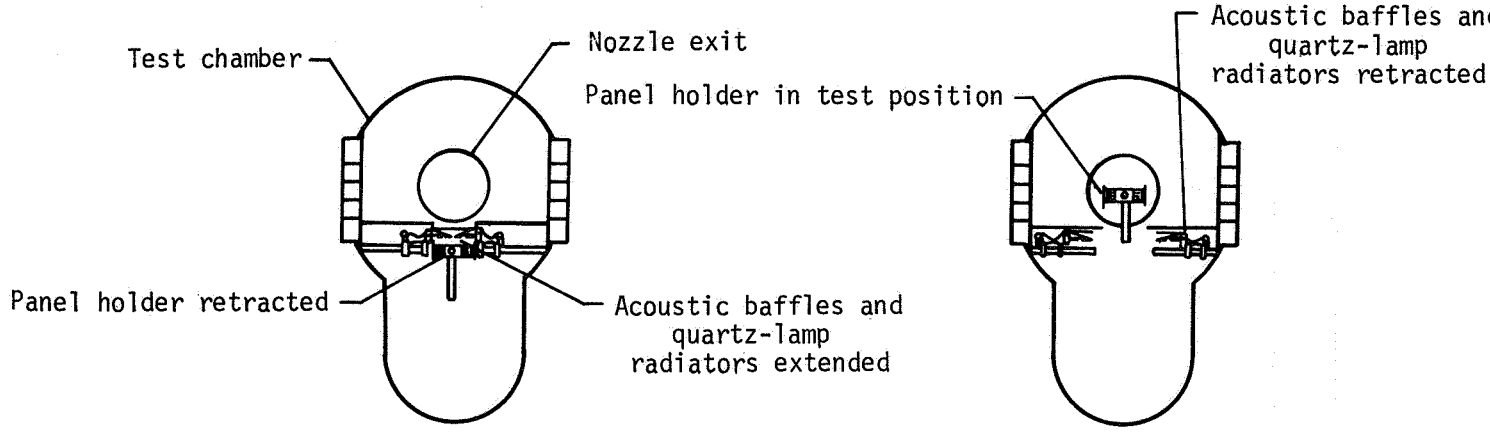

(b) Model position during preheat.

(c) Model position during test.

Figure 14.- Schematic of Langley 8-Foot High-Temperature Structures Tunnel. Dimensions are in meters.

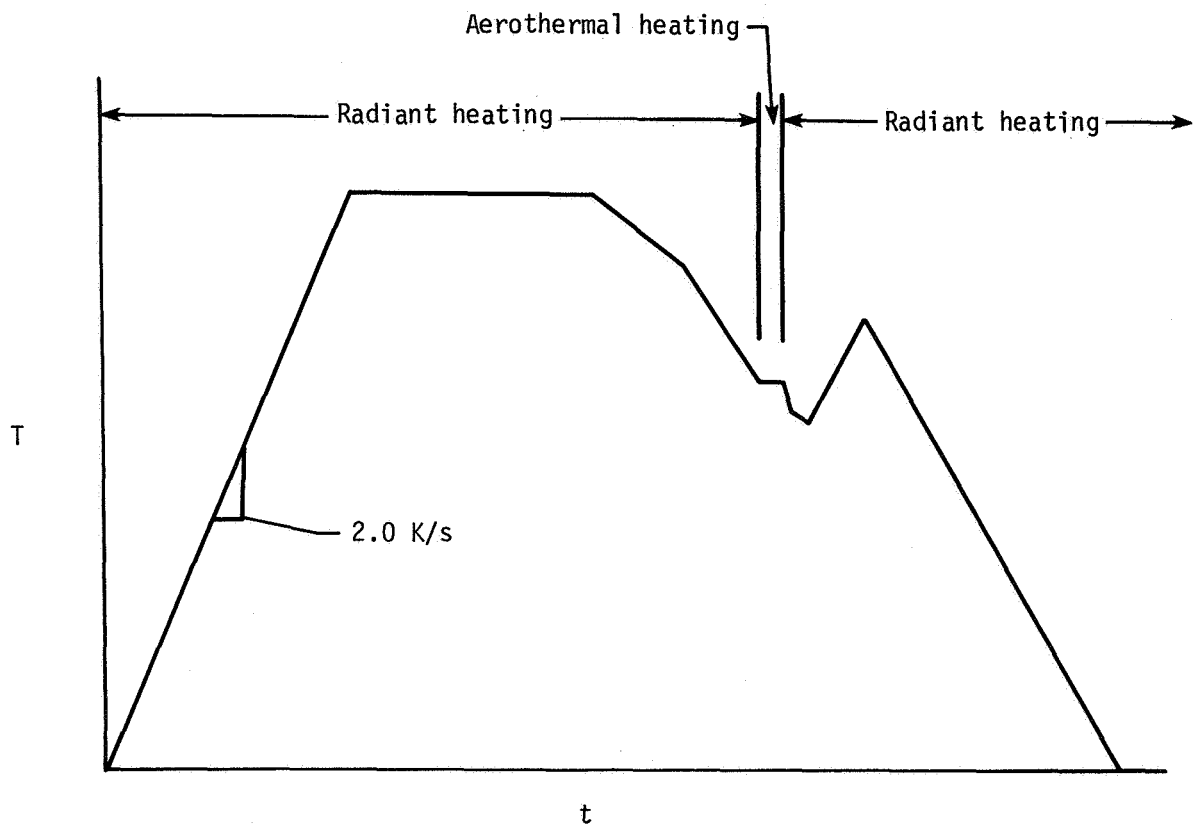

Figure 15.- Typical radiant or radiant preheat/aerothermal surface heating profile for Space Shuttle reentry conditions. (Aerothermal heating section deleted during radiant heating tests.)

Ra Radiant heating tests
A Radiant preheat/aerothermal tests

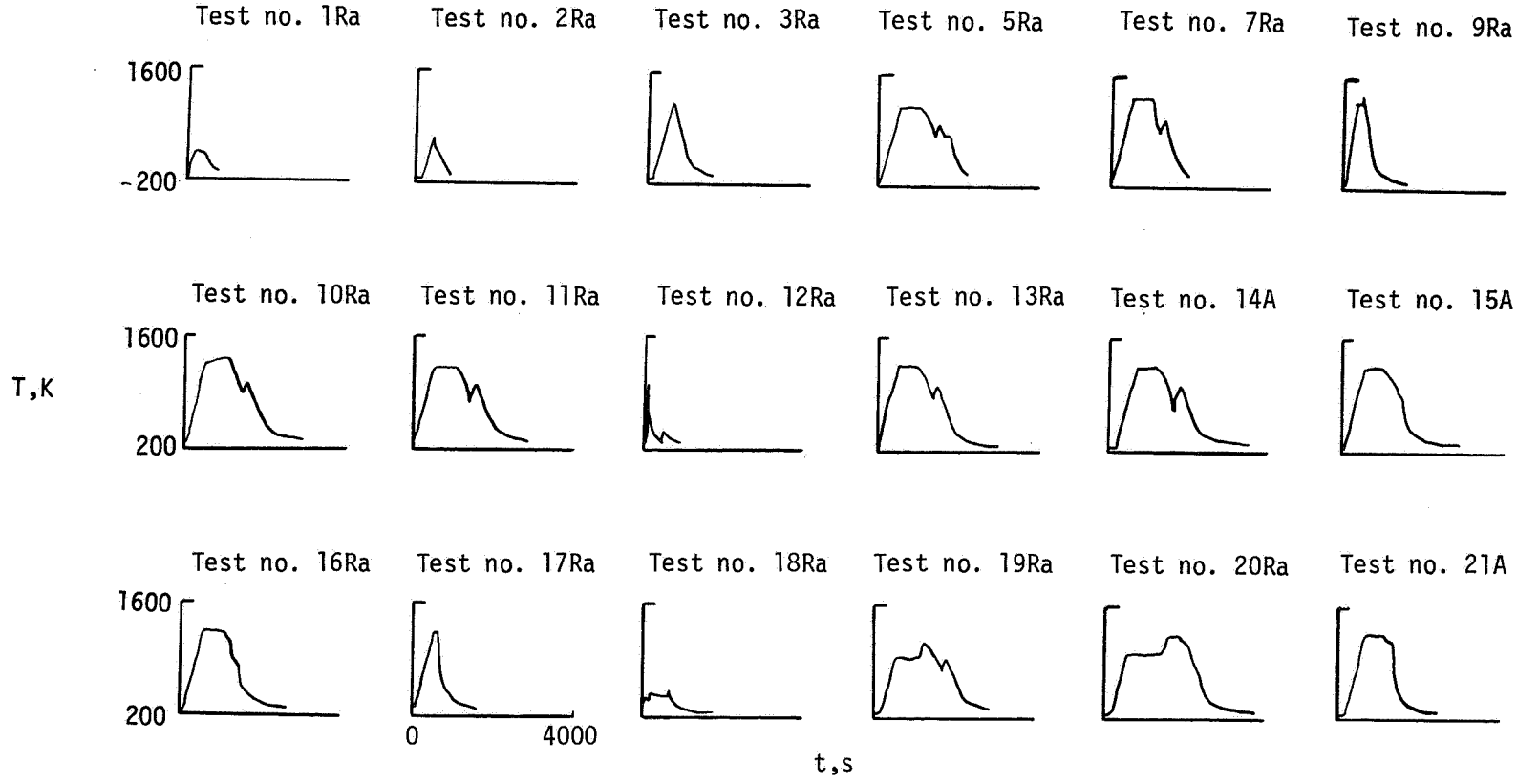

Figure 16.- Surface temperature histories.

Ra Radiant heating tests
A Radiant preheat/aerothermal tests
P Δp checkout

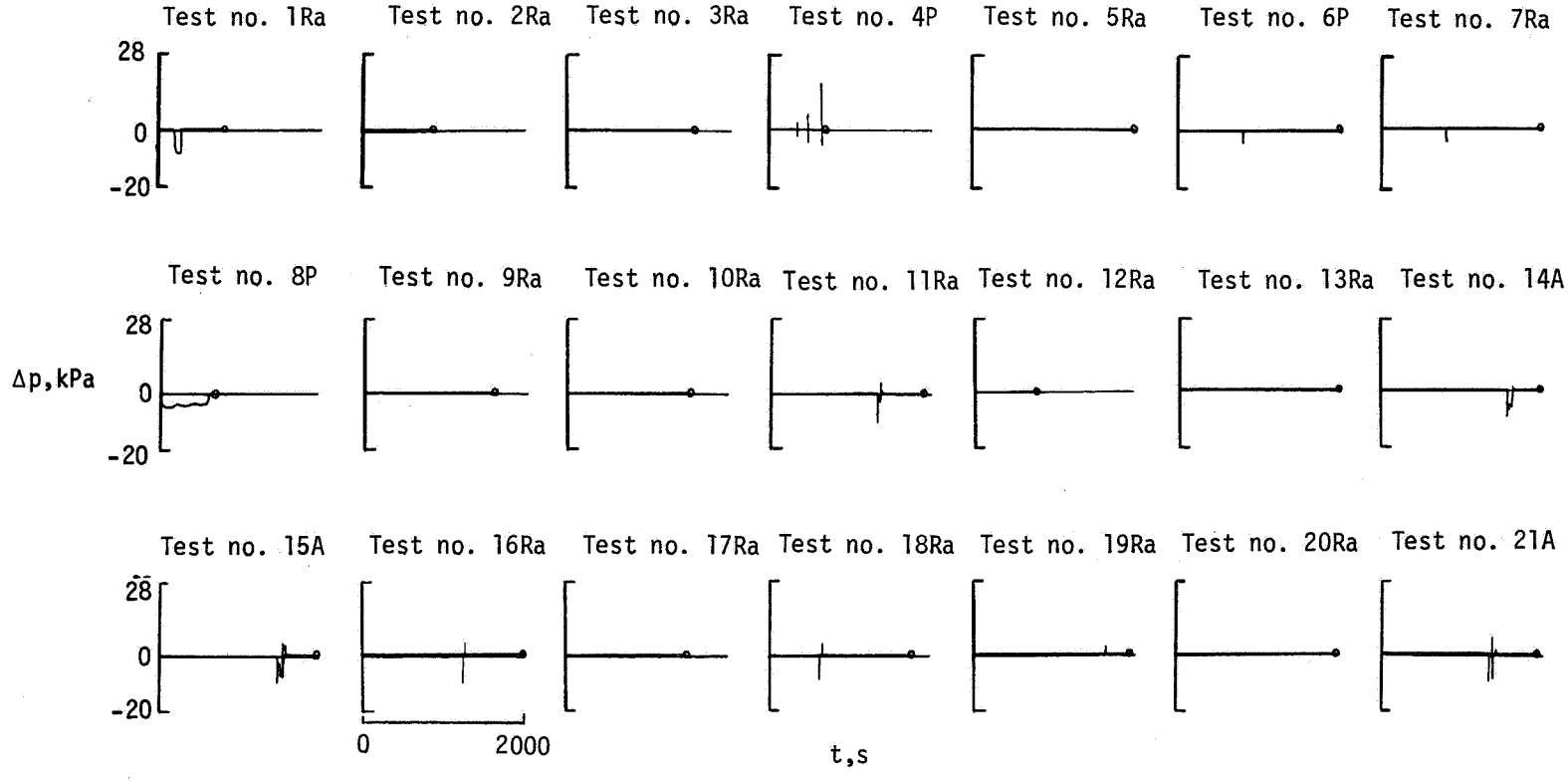

Figure 17.- Differential pressure histories.

Ra Radiant heating tests
A Radiant preheat/aerothermal tests
P Δp checkout

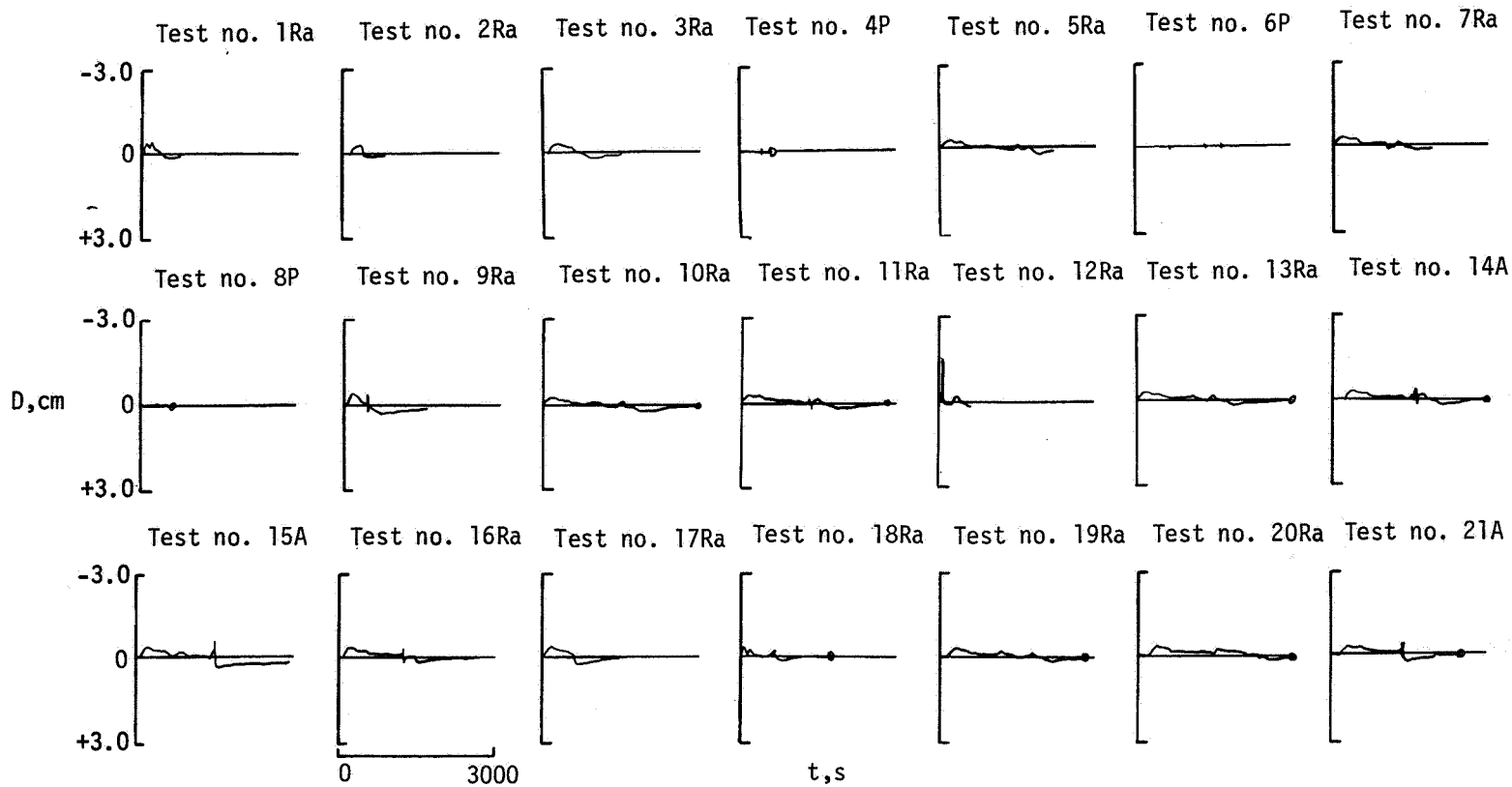

Figure 18.- Surface deflection histories.

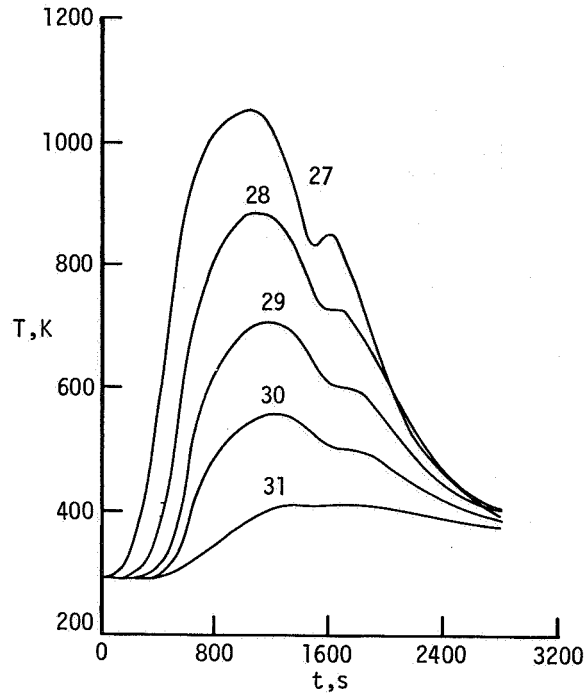

(a) Test 11 (radiant test).

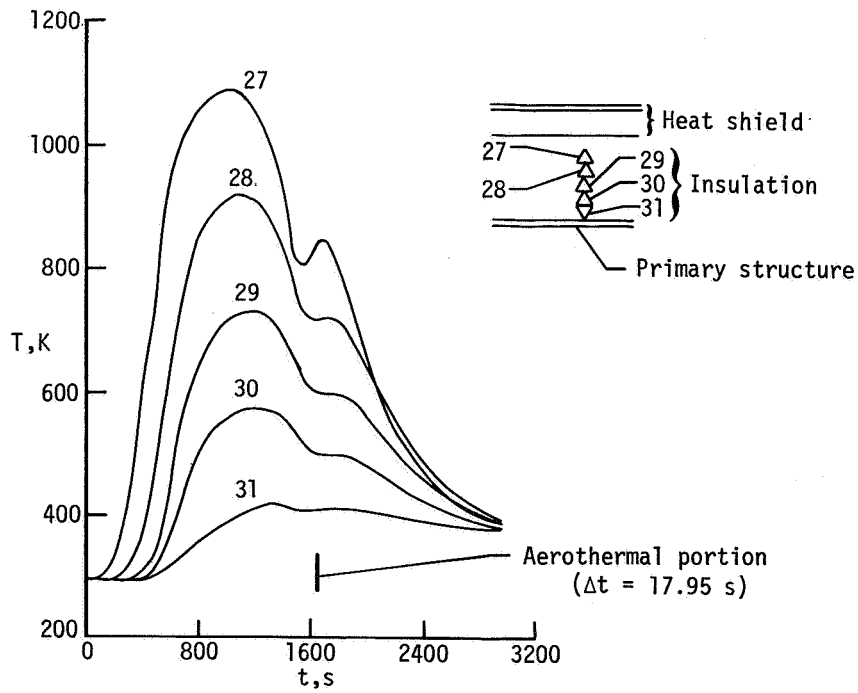

(b) Test 14 (aerothermal test).

Figure 19.- Temperature distribution through insulation.

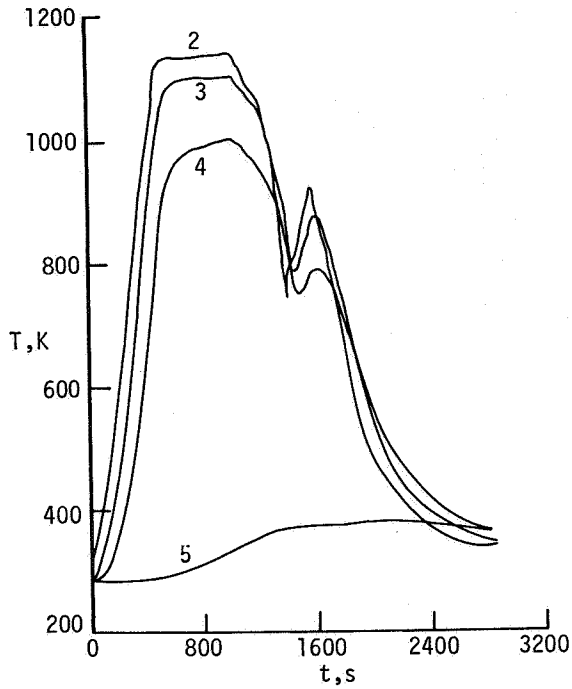

(a) Test 11 (radiant test).

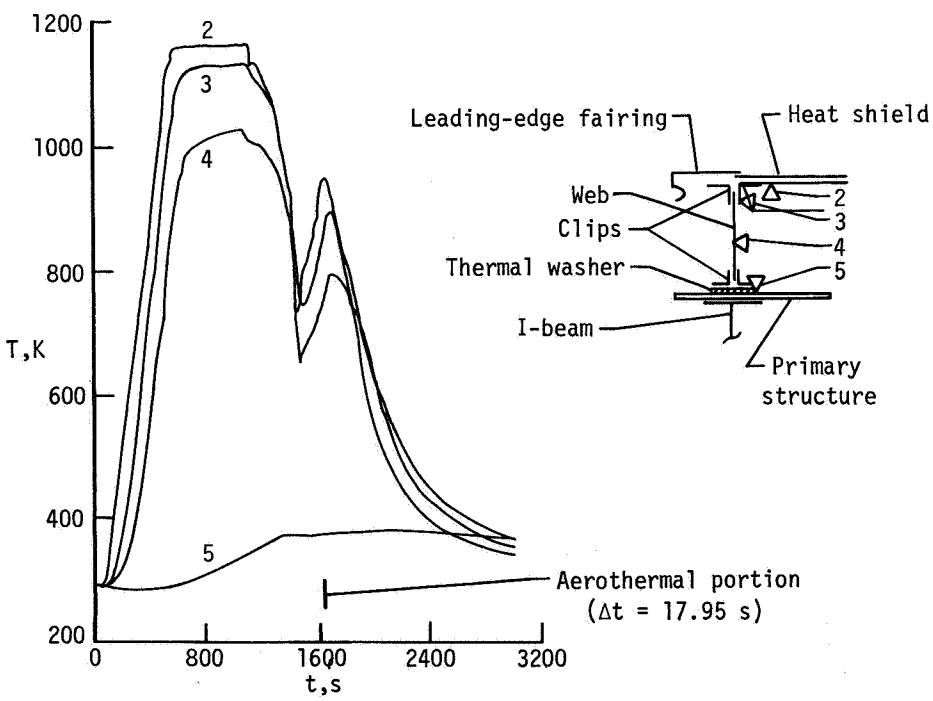

(b) Test 14 (aerothermal test).

Figure 20.- Temperature response of heat shield, support, and primary structure.

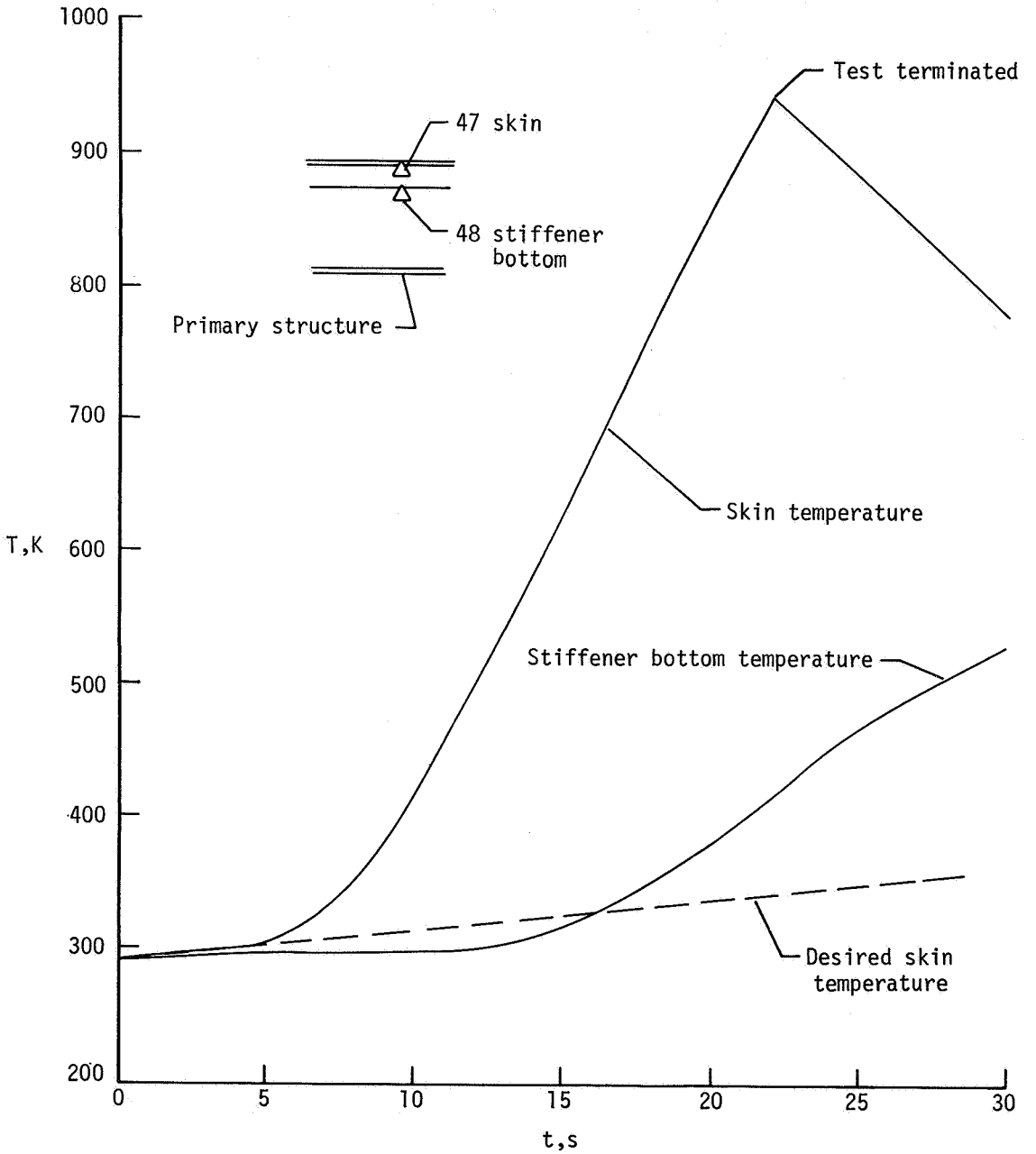

Figure 21.- Temperature profile for test 12.

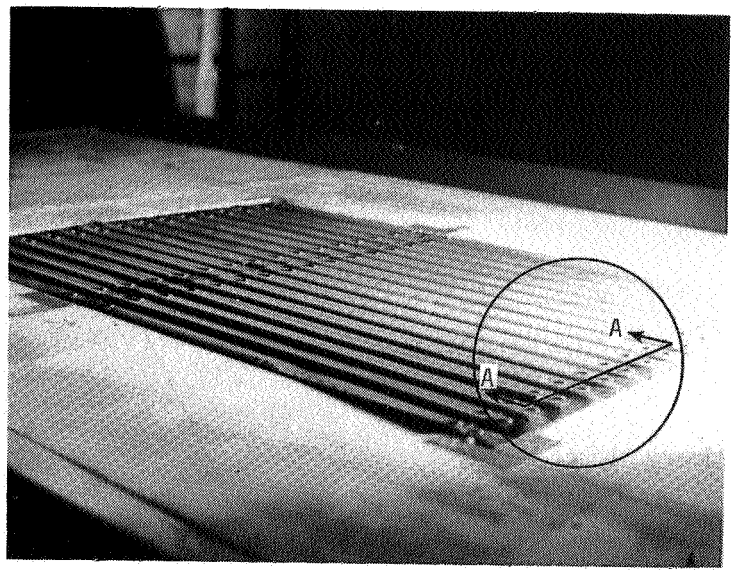

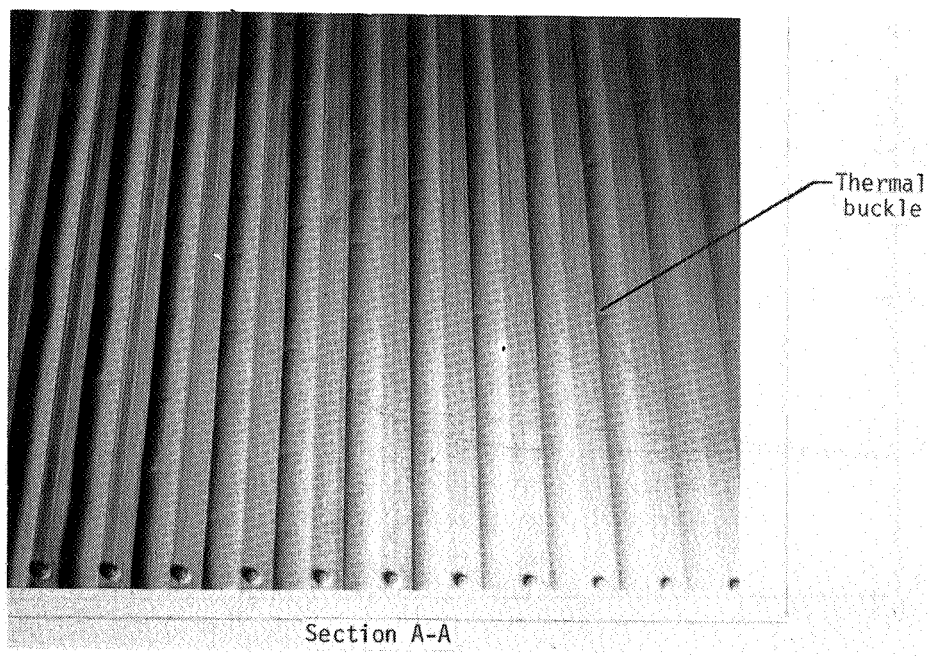

L-81-108

Figure 22.- Thermal buckling.

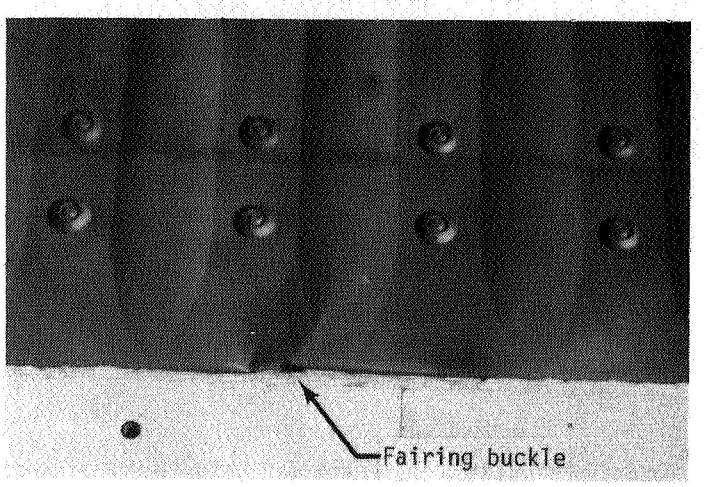

(a) Leading-edge fairing crack soon after development.

(b) Leading-edge fairing failure.

L-81-109

Figure 23.- Haynes 188 TPS model leading-edge fairing failure.

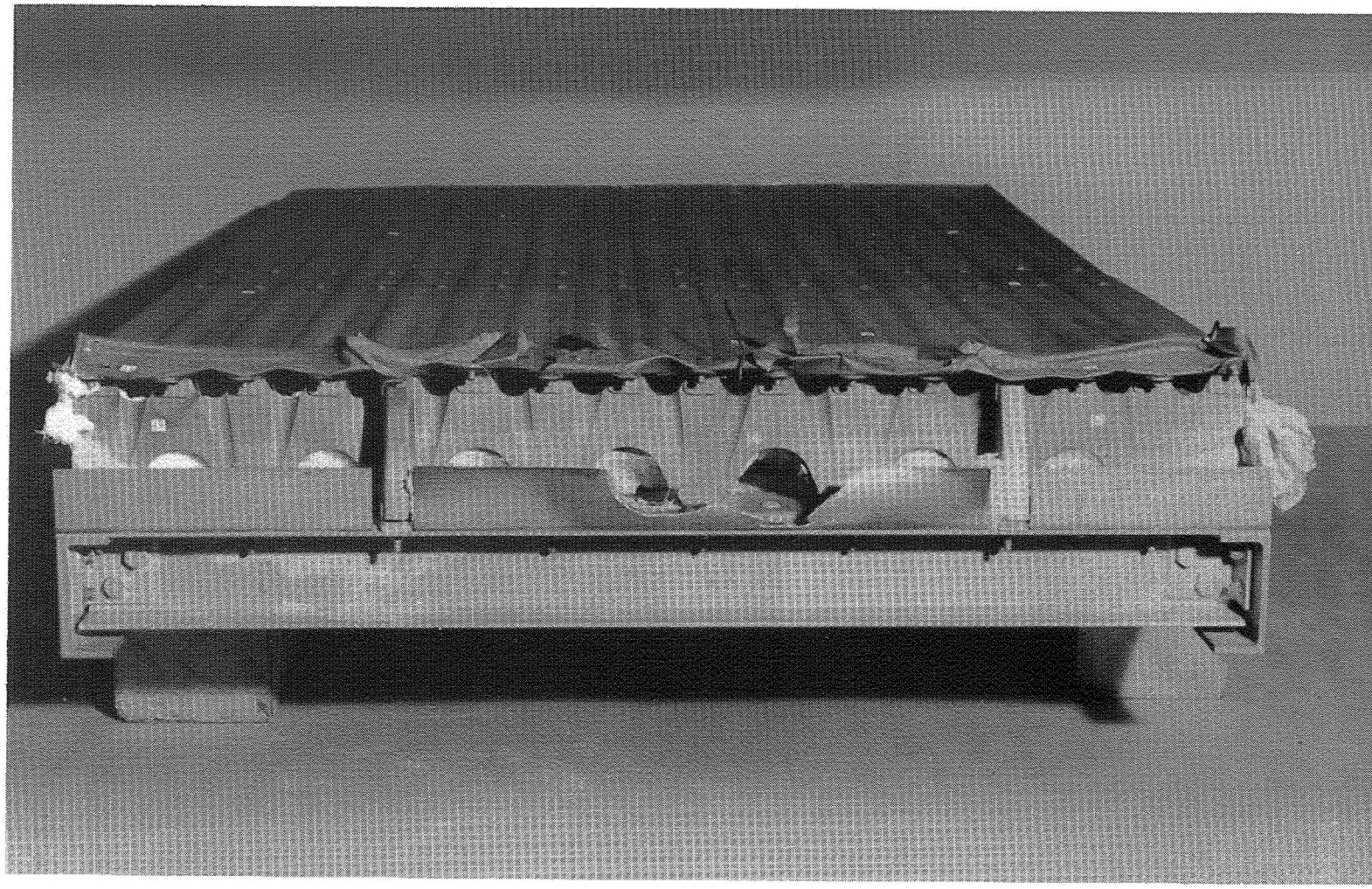

L-81-110

(c) Front view of leading-edge fairing failure.

Figure 23.- Continued.

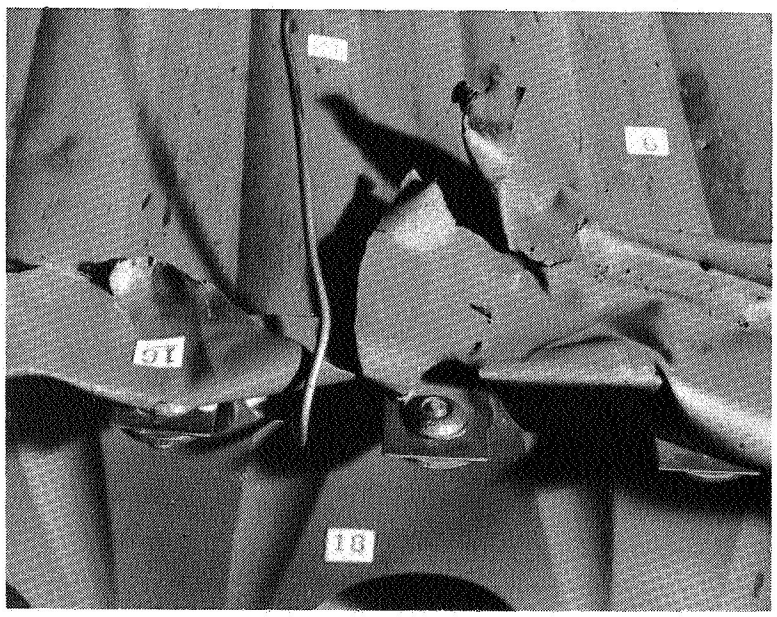

(d) Leading-edge fairing damage in area of crack.

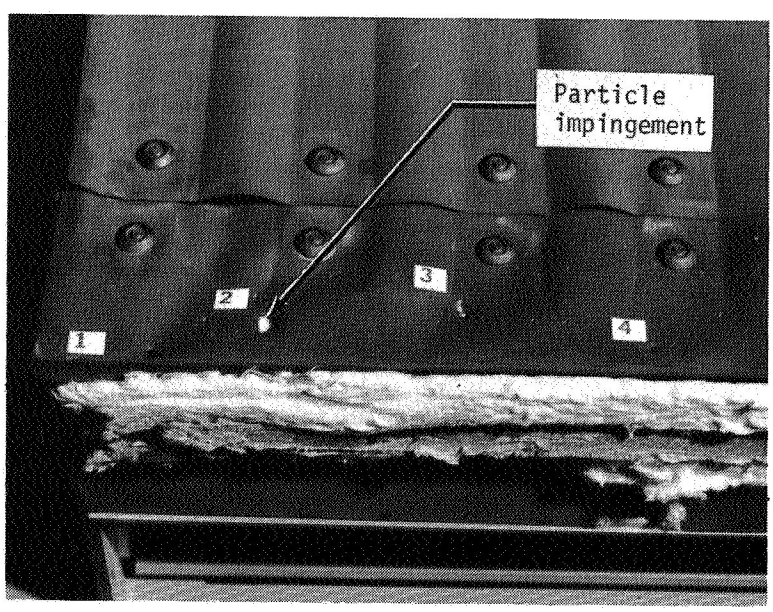

(e) Trailing-edge fairing damage.

L-81-111

Figure 23.- Concluded.

1. Report No.	2. Government Accession No.	3. Recipient's Catalog No.
NASA TP-1802		

4. Title and Subtitle	5. Report Date
PERFORMANCE OF A HAYNES 188® METALLIC STANDOFF THERMAL PROTECTION SYSTEM AT MACH 7	April 1981
	6. Performing Organization Code 533-01-13-06
7. Author(s)	8. Performing Organization Report No.
Don E. Avery	L-13903
	10. Work Unit No.
9. Performing Organization Name and Address	
NASA Langley Research Center Hampton, VA 23665	11. Contract or Grant No.
	13. Type of Report and Period Covered
12. Sponsoring Agency Name and Address	Technical Paper
National Aeronautics and Space Administration Washington, DC 20546	14. Sponsoring Agency Code

15. Supplementary Notes

16. Abstract

A flight-weight, metallic thermal protection system (TPS) model applicable to reentry and hypersonic vehicles was subjected to multiple cycles of both radiant and aerothermal heating to evaluate its aerothermal performance and structural integrity. The TPS was designed for a maximum operating temperature of 1255 K and featured a shingled, corrugation-stiffened corrugated-skin heat shield of Haynes 188®, a cobalt-base alloy. Tests were conducted in the Langley 8-Foot High-Temperature Structures Tunnel. The model was subjected to 3 radiant preheat/aerothermal tests for a total of 67 seconds and to 15 radiant heating tests for a total of 85.9 minutes at 1255 K. The TPS limited the primary structure to temperatures below 430 K in all tests. No catastrophic failures occurred in the heat shields, supports, or insulation system. The TPS continued to function even after exposure to a differential temperature 4 times the design value produced thermal buckles in the outer skin. The shingled thermal expansion joint effectively allowed for thermal expansion of the heat shield without allowing any appreciable hot gas flow into the model cavity, even though the overlap gap between shields increased after several thermal cycles.

17. Key Words (Suggested by Author(s))	18. Distribution Statement
Thermal protection system (TPS) Haynes 188® Space Shuttle Orbiter	Unclassified - Unlimited Subject Category 18

19. Security Classif. (of this report)	20. Security Classif. (of this page)	21. No. of Pages	22. Price
Unclassified	Unclassified	41	A03

For sale by the National Technical Information Service, Springfield, Virginia 22161